

https://dspace.org/

Corrosion resistant materials in highpressure hightemperature oil wells An overview and potential application of complex concentrated alloys

Desmond Klenam; F Mcbagonluri; Olufemi Bamisaye; T.K Asumadu; N.K Ankah ...

PERGAMON-ELSEVIER SCIENCE LTD
https://hdl.handle.net/10539/40508
WOS

Downloaded from a DSpace repository. https://dspace.org/

Engineering Failure Analysis 157 (2024) 107920



Contents lists available at ScienceDirect

Engineering Failure Analysis

journal homepage: www.elsevier.com/locate/engfailanal

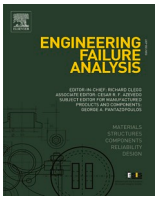



Corrosion resistant materials in high-pressure high-temperature oil wells: An overview and potential application of complex concentrated alloys

D.E.P. Klenam [a,b,c,*], F. McBagonluri [d], O.S. Bamisaye [b,e], T.K. Asumadu [f], N. K. Ankah [g], M.O. Bodunrin [b], A. Andrews [h], W.O. Soboyejo [i]

[a] Academic Development Unit, Faculty of Engineering and the Built Environment, University of the Witwatersrand, Johannesburg, South Africa
[b] School of Chemical and Metallurgical Engineering, University of the Witwatersrand, Johannesburg, South Africa
[c] Africa Oxford Fellow, Oxford Micromechanics Group, Department of Materials, University of Oxford, Oxford, UK
[d] Office of Provost and President, Academic City College, Haatso, Accra, Ghana
[e] Mechanical Engineering Department, Air Force Institute of Technology, Kaduna, Nigeria
[f] Department of Materials Engineering, Sunyani Technical University, Sunyani, Ghana
[g] Centre of Research Excellence in Corrosion, King Fahd University of Petroleum and Minerals, Dhahran 31261, Saudi Arabia
[h] Department of Materials Engineering, Kwame Nkrumah University of Science and Technology, Kumasi, Ghana
[i] College of Engineering, SUNY Polytechnic Institute, 100 Seymour Street, Utica, NY 13502, USA

ARTICLE INFO

Keywords:
Complex concentrated alloys
Sweet and sour corrosion
Sulphide stress cracking
Corrosion resistant alloys
Cost of corrosion

ABSTRACT

This review discusses potential applications of complex concentrated alloys (CCAs) for mitigating sweet and sour corrosion in high-pressure, high-temperature (HPHT) wells with concentrated chlorides, carbon dioxide and hydrogen sulphide. The harsh oil and gas environments lead to severe components failures through sour corrosion, sweet corrosion, hydrogen induced cracking, stress corrosion cracking and corrosion fatigue. Many of these failures are material driven. Hence the domain of complex concentrated alloys are being explored to reduce the severity of failures in the oil and gas industry, especially in HPHT zones. The CCAs possess high thermal stability, the balance of strength and ductility resulting from complex deformation mechanisms, and high creep resistance due to sluggish diffusion. These properties are driven by the design philosophy: high entropy and enthalpy of mixing, severe lattice distortion, sluggish diffusion, chemical ordering, and the cocktail effects. These effects allow for greater flexibility and many degrees of freedom which is absent in conventional one principal element-based materials. Most CCAs have shown excellent and superior mechanical and corrosion properties in some of the environments of currently used corrosion-resistant alloys in the oil and gas industry. This review highlights recent literature on potential high entropy alloy chemistries, microstructural features and their effects on mechanical and corrosion properties, and areas for future research directions.

* Corresponding author at: Academic Development Unit, Faculty of Engineering and the Built Environment, University of the Witwatersrand, Johannesburg, South Africa.
E-mail address: desmond.klenam@wits.ac.za (D.E.P. Klenam).

https://doi.org/10.1016/j.engfailanal.2023.107920
Received 12 September 2023; Received in revised form 7 December 2023; Accepted 25 December 2023
Available online 5 January 2024
1350-6307/© 2023 The Author(s). Published by Elsevier Ltd. This is an open access article under the CC BY-NC-ND license (http://creativecommons.org/licenses/by-nc-nd/4.0/).

1. Introduction

Oil and gas are fossil fuels from dead and decayed flora and fauna within the marine and aquatic environment after millions of years. These decayed fauna and flora are randomly distributed within rocks due to increased pressure and temperature beneath the ocean floor. The rocks contain crude oil, gas and water arranged in order of increasing densities with significant transition zones based on phase mixing. Although the water does not displace the oil or the gas during the reservoir formation, it wets the walls of the rock pores forming a film, which aids oil flow during production. Within these reservoirs, temperatures are above 200 °C and pressures above130 MPa (~1300 atmospheres) [1]. Aside elevated temperatures and pressures, high reactive species, and gases such as CO_2 and H_2S make this environment very harsh and aggressive to materials. These are sweet (CO_2) and sour (H_2S) environments [2–13].

Energy demands globally have skyrocketed due to the increasing human population (~8.1 billion). This has adverse impact on natural resources resulting in the exponential depletion of most proven oil and gas reserves [2,3,4]. In 2018, global energy demand increased about twice the average of the last decade, with ~ 45 % being natural gas. Natural gas is expected to reach 5400 billion cubic meters by 2040, which would be greater than the 40 % it was in 2018. Similarly, oil demands are expected to reach 106 million barrels per day (Mb/d) by 2040 from the 97 Mb/d observed in 2018. Renewable energy technologies have tripled over the last three decades but are a bite-sized chunk of the total energy mix. Proven reserves have ~ 90 % of profit recovery, whereas unproven reserves are considered high risk, plagued with uncertainty and massive engineering challenges. Increasing demand for oil and gas has necessitated the exploration of unproven reserves and high-pressure high-temperature (HPHT) fields. These reserves require innovative technologies, new methodologies, and advanced materials with superior functional and structural properties [2].

Mitigation measures are based on bulk alloy design, coatings, corrosion inhibitors and cathodic protection. These approaches are used to reduce the severity of materials degradation and the effects of corrosion in the oil and gas sector. However, many of these approaches and current corrosion resistant alloys are ineffective in HPHT wells. Corrosion resistant alloys (CRAs) being used in proven reserves are Ti-based alloys, low-alloy steels, duplex and super duplex steels and ferritic-martensitic stainless steels [2,4–15]. Corrosion inhibitors are applied under low temperatures mostly up to 100 °C beyond which they become chemically unstable and ineffective [16,17]. The HPHT wells also require materials with superior yield strength exceeding 690 MPa, ductile to brittle transition temperatures (DBTTs) below ~ -60 °C and adequate sour and sweet corrosion resistance [4]. Sadly, the corrosion resistance of the steel pipes in the HPHT wells has not been great nor have corrosion inhibitors been effective [18]. Regardless of the remedial actions of CRAs, the pervasive and aggressive HPHT wells lead to severe environmentally assisted cracking (EAC) including stress corrosion cracking (SCC), corrosion fatigue (CF) and hydrogen induced cracking (HIC) [4,19].

The cost of corrosion globally is about 2.5 trillion annually, ~3.4 % of the gross domestic product (GDP) of the world. In the oil and gas sector, a quarter of all failure cases are corrosion-related, and more than half are associated with sweet (CO_2) and sour (H_2S) producing fluid [16,20,21]. For unproven reserves, apart from the devastating elevated temperatures and pressures, the crude also contains up to 10 % H_2S, 4 % CO_2 and elemental Sulphur, ~50 % higher than the proven wells [2,3,4,18]. Due to high depths of ~ 1800 m, there is high concentration of chlorides, extremely reactive mercury species and very high partial pressures of carbon dioxide and hydrogen sulphide, increasing the rate of metal dissolution and corrosion rates [3]. Due to the extremely aggressive and harsh nature of these carbon and sulphur-based environment, carbon steels being used are susceptible to stress corrosion cracking (SCC) and hydrogen induced cracking (HIC). In cases where austenitic stainless steels are used, in-service grain boundary precipitation is prevalent, leading to sensitization (intergranular) corrosion [22]. Considering that over 90 % of production equipment are made from carbon steels which are less resistant to oxidation, corrosion will continue to persist.

Traditional alloy development strategies require the addition of minute secondary elements to complement the properties of the base element [23]. The alloying elements induced the desired and designed properties, an alloy design strategy which have lasted for centuries. In the last decade and a half, alloy design paradigms have shifted to using equimolar or near equimolar amounts of five to seven elements, leading to complex concentrated alloys [24,25]. This multi-principal elements approach (with a high concentration of 5–35 wt%) has extended the compositional space for alloy design and gaining traction over conventional alloys [23].

The drive for the oil and gas sector is to increase yield and overall plant operability. This is attainable by reducing increased operating expenses from unplanned maintenance and intermittent shutdown due to breakdown of machinery and corrosion-induced failures. Methods and systems need to be developed to increase production throughput. One of such is the need for low-cost bulk corrosion-resistant complex concentrated alloys and coatings than currently used ferrous based alloys and coatings for the different grades and types of crude. These new classes of alloys are expected to perform well in sulphur and carbon dioxide containing wells. Some of the key parameters affecting sweet and sour corrosion mechanisms in traditional oil and gas environments have been highlighted [26–31]. Generally, the effects on mechanical components are dire and ~ 60 % of internal corrosion of pipelines transporting crude is attributed to dissolution of CO_2, H_2S and other reactive gases, compromising structural integrity [27]. Thus, the need for the design and application of next generation corrosion resistant alloys is warranted. This window of opportunity falls in the domain of complex concentrated alloys – paradigm shift in alloy design.

Based on the design paradigm of CCAs, these alloys are expected to be applicable to wide range of design parameters such as strength, toughness, fatigue strength, wear and corrosion resistance. Recent CCAs have shown better corrosion and pitting resistance than different classes of hypoeutectoid, hypereutectoid carbon and stainless steels, which are widely used in the oil and gas sector [32–36]. There are authoritative reviews of corrosion resistant behaviour of composition-based and microstructural-driven CCAs across various industries [32,33,36–46]. These comprised of bulk materials and coatings where different techniques have been used to deposit low-cost CCA-based coatings on various substrates. For instance, the 304 austenitic stainless steel substrate is coated with CCA to improve corrosion and cavitation erosion resistance [47].

In this review, corrosion resistance of conventional alloys used in HPHT environments are compared with some promising complex

concentrated alloys (CCAs). The need for oil and gas exploration at high pressure and high temperature ranges has become critical. This is due to less exploitation of crude oil and natural gases in most HPHT environment and continuous dependence on fossilized fuel with increasing population growth globally. The effect of the processing route (mechanical alloying, laser melting and arc melting) on microstructures and the electrochemical polarisation behaviour of CCA are briefly discussed. The potential for the application of complex concentrated alloys in the high-pressure high temperature oil wells are discussed. Areas for further research directions and implications are then highlighted briefly. The implication of this review for robust design of next generation corrosion resistant CCAs are briefly discussed.

2. Aggressive and harsh environment in the oil and gas industry

The oil and gas industry is high risk with highly flammable and noxious chemical substances injurious to health and the environment [48]. The prevalence of corrosion in the oil and gas industry is due to the physicochemical properties of reactive gases and substances. These include different mixes of hydrocarbons, dissolved gases (e.g. carbon dioxide, hydrogen sulphide, nitrogen, oxygen), water, salt, and other reactive contaminants, e.g., metals, with distinct phases [18]. Crude is a product of decayed flora and fauna, hence residues of these micro-organisms form part of it. Aqueous substances (e.g., water and salt solutions) in crude vary from fresh to saturated, the main corrosive electrolyte for the electrochemical reaction cell.

The composition of natural gas is a mixture of gaseous hydrocarbons with N_2, H_2S, H_2O, CO_2, organic acids, and traces of mercury. Apart from N_2, the rest are corrodents. The cumulative effects of these reactive gaseous species and contaminants are precursors for the prevalence of sour and sweet corrosion in the oil and gas industry [18,48]. Carbon dioxide and H_2S dissolve in the wells forming weak acids which easily corrode the steel structures. The oxygen content of natural gas is responsible for typical oxygen corrosion. Sweet and sour corrosion occurs within the wells, whereas external corrosion of the wells is due to oxygen presence. Although, sour and sweet corrosion mechanisms are complicated and complex, hydrogen sulphide and carbon dioxide are critical to the severity of the corrosion behaviour [18,48]. The corrosion rate and its intensity is dependent on temperature and the pressure (concentration) of the reactive species, flow regime and velocity [18]. Thus, deep wells (above 1000 m) are very harsh and aggressive corrosive environments due to the high pressures (68 MPa) and extreme temperatures (>150 °C). Based on temperature and pressure three distinct zones have been defined for oil wells (Table 1). These are the high-pressure (HP) (>69 MPa) high-temperature (HT) (150 °C) wells, ultra – HPHT (>205 °C and > 138 MPa) and HPHT that are highly critical (HPHT - HC) wells (>241 °C and > 260 MPa).

3. High-pressure high-temperature environments and challenges

As proven reserves onshore and offshore are depleting, very deep wells (>1000 m) are being drilled and explored. Drilling deep into the Earth comes with the challenge of reaching the elevated temperatures and pressure domains. The term high-pressure high-temperature (HPHT) in oil and gas exploration was coined in 1990, but the first HPHT drilling was in 1965 in Mississippi with depth reaching 6000—–6900 m and pressures of 120–150 MPa [50]. The American Petroleum Institute API PER 15 K Code defines HPHT wells as having minimum seabed pressures of 103 MPa and temperatures exceeding 120 °C [51]. The seabed pressure of 103 MPa changed to 137 MPa in 1972, then to 200 MPa in 1974. Successful systems were deployed and commissioned in land and platform-based fields in the Gulf of Mexico and the North Sea under such conditions [52]. Wells for high viscosity crude fall under HPHT as they are operated using steam-assisted gravity-drainage (SAGD) to increase temperatures for easy operations. Similarly, geothermal wells are also considered HPHT due to the exceedingly high operating pressures. A typical well designation based on pressure and temperature is given in Fig. 1 [49].

Many HPHT wells exist in Africa, Southeast Asia, China, the Middle East, South America, the North Sea, and the Gulf of Mexico. The increasing temperature and pressure meant an aggressive and harsh corrosive environment. Apart from severe cement challenges leading to a reduction in concrete stability and compressive strength, HPHT crude contains up to 10 % H_2S, 4 % CO_2 and elemental sulphur, which promote sour and sweet corrosion mechanisms [50]. About 25 % of failure cases in the oil and gas industry are corrosion-related whereas over 50 % are associated with sweet (CO_2) and sour (H_2S) producing fluids [53]. In the sour environment, H_2S reduces the pH of the environment and then acts as a catalyst for the penetration of hydrogen atoms into the conventional structural steels (carbon, low-alloy and stainless steels). The hydrogen atoms then embrittles the structural steel, resulting in mechanically assisted cracking (MAC) [2,4]. Other classes of conventional alloys are the Ti-based and Ni-based alloys. Major materials that pose great concerns are the tieback casing string and liners at the bottom of the wells.

The other forms of corrosion in HPHT domain are the general corrosion and localised corrosion in the oil and gas industry [54,55]. The general corrosion in HPHT is a uniform attack due to corrosive fluids (high concentration of dissolved salts) and highly acidic and reactive gases. Structures produced from carbon steels with low corrosion resistance are susceptible. The different types of localised corrosion in oil and gas industry, and under HPHT conditions are shown in Fig. 2 [55]. Defective sites such as minute cavities and

Table 1
Category of oil wells based on pressure and temperature ranges [49].

Oil well categories	Pressure (MPa)	Temperature (°C)
High pressure and high temperature	> 69	>150
Ultra-high pressure and high temperature	> 138	>205
HPHT – HC (highly critical)	>241	>260

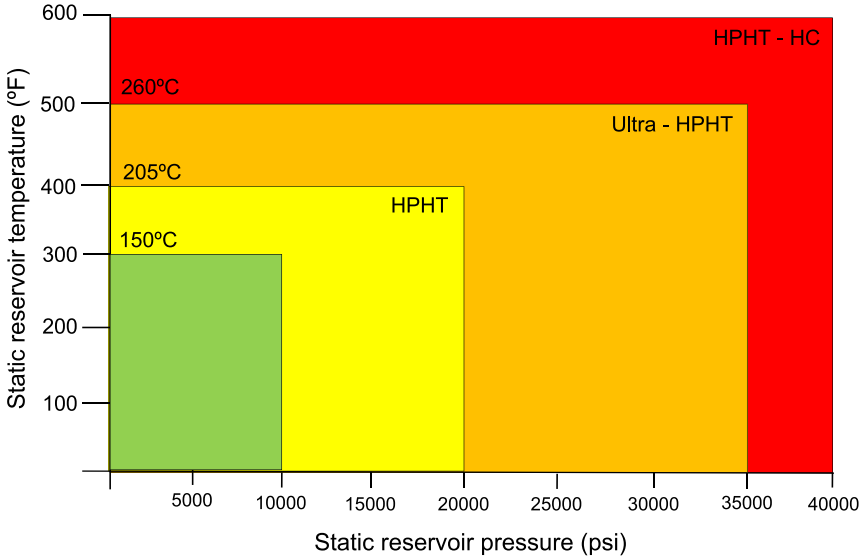

Fig. 1. Oil and gas well based on temperature and pressure profile. (HC – highly critical) [49].

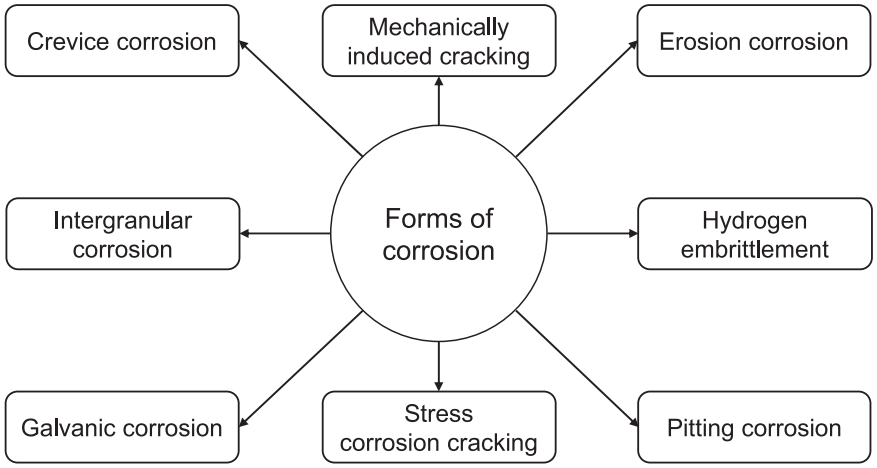

Fig. 2. Localised corrosion types in the oil and gas industry [55].

cracks provide favourable pathways for the process to take place in the presence of sulphides, chlorides and other aggressive reactive species. Scaling is another prevalent corrosion behaviour in HPHT environments. This is a complex process of salt-forming compounds and other easily dissolvable minerals in the crude precipitates on the structural material. This forms scale deposits and then accumulate with time resulting in reduced flowrate of the crude. This process promotes pressure build up throughout the structure acting as stress raisers and can lead to other forms of material degradation.

4. Corrosion in the oilfield environment

Corrosion has devastating effects on society, causing the deterioration of household appliances and industrial equipment. It has direct and indirect costs leading to loss of productive time due to downtime, delays, intermittent shutdowns, and overheads. Corrosion cost is estimated at ~ 3–5 % of the gross domestic product of industrialised economies. For the oil and gas sector, corrosion is the main factor affecting structural integrity, the shelf life of mechanical components and the reliability of operations [5–8]. In the United States, there are over 528,000 km of natural gas transmission and gathering lines, ~119,000 km for crude transmission and ~ 132000 km for hazardous liquids. An estimated $7 billion is required annually to assess, monitor, and maintain these assets, with 80 % of the cost due to corrosion. The cost of corrosion in the United States per five major sectors of the economy is shown in Fig. 3. Utilities and transportation cumulatively account for over 50 %.

Corrosion in oilfields occur in pipelines, drilling equipment and storage tanks [5–8,56–63]. This is due to highly aggressive and

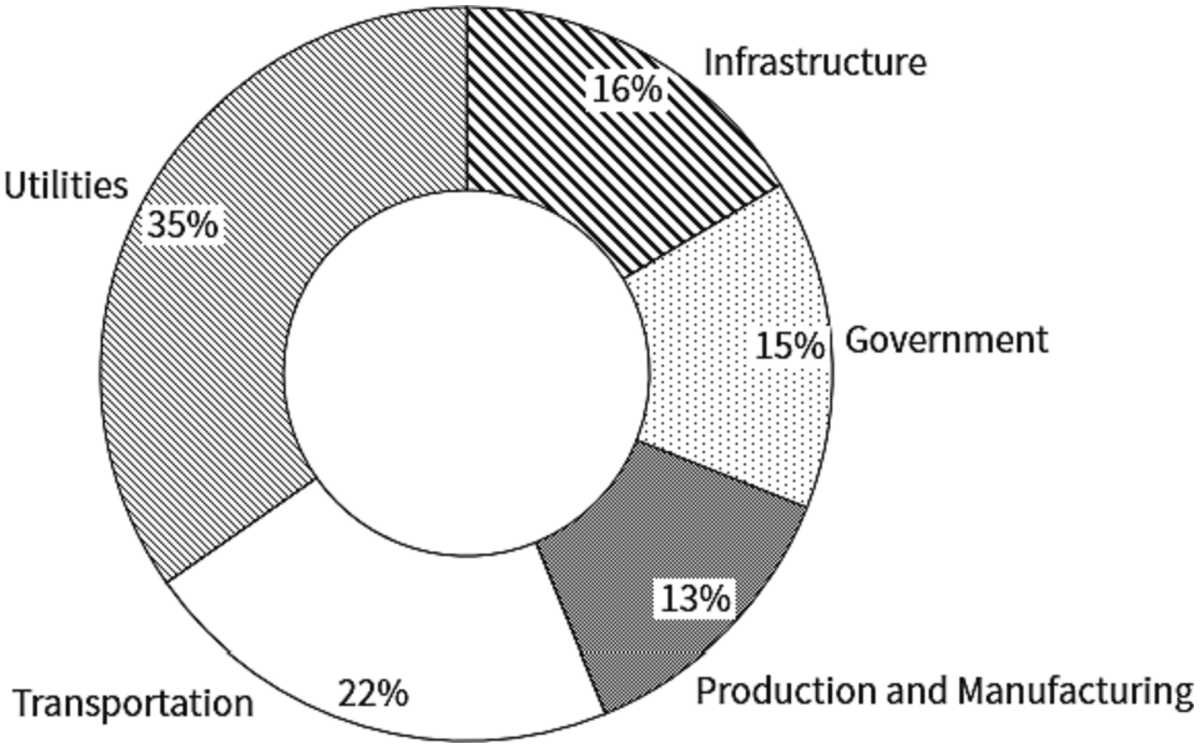

Fig. 3. Sectors of the US economy and cost of corrosion prevention and control [69].

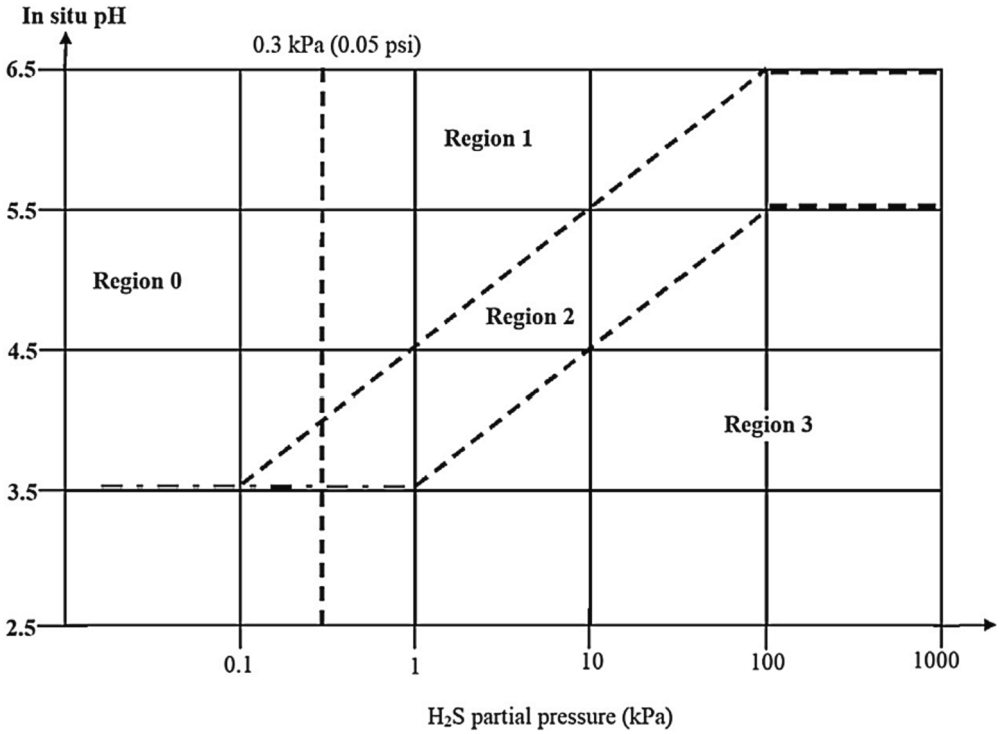

Fig. 4. The "region of service" for sour conditions according to NACE MR0175/ISO 15156 [74].

corrosive nature of these environment with complex reactive species and contaminants such as salts, water and gases [59–63]. These factors are critical for accelerating the electrochemical processes which induces the severity of corrosion process. Furthermore, saline, acidic, high pressures and high temperatures are also severe contributing factors to the corrosion process. Depending on the conventional materials (carbon steel, low alloy steels, stainless steels, Ti-based alloys and Ni-based), common forms of uniform, pitting, galvanic and crevice corrosion are eminent [59–63]. According to North American Pipeline and Hazardous Materials Safety Administration (PHMSA), failure of Oil and Gas infrastructure due to corrosion and material related accounted to more than 60 % from 2009 to 2018 [62]. More than 17 % were corrosion-related.

Corrosion of oilfield infrastructure is in two folds: externally around the wells and internally in the wells [60–62]. Externally driven corrosion is attributed to dissolved oxygen from groundwater and seawater around the immersed infrastructure which undergoes oxidation [53,56,64–67]. The dissolved oxygen is reduced to hydroxide ions using the excess electrons produced from the anode to balance the electrochemical circuit. Internal corrosion mechanisms are based on the "sourness" and "sweetness" of the crude [27,63,68].

In the oil and gas industries, sour conditions are found in unconventional reservoirs. An example is the shale gas formations which are at very deep depth with high sulphur contents. Factors such as sulphur reducing bacteria, moisture, oxygen, H_2S concentration, pressure and temperature are the main contributing factors to the sour corrosion mechanisms. Sweet conditions are located at shallow depths of conventional reservoirs with relatively low sulphur contents. Generally, sweet conditions are relatively better and are less corrosive than most sour conditions [64]. Although, sweet and sour corrosion conditions are seldom separable, there is always one form dominating. This is due to the presence of many gaseous and ionic species in oilfield brines. These include dissolved carbon dioxide, carbonic acid, bicarbonate ion, carbonate ion, H^+, OH^-, Cl^-, Na^+, K^+, Mg^{2+}, Ca^{2+}, Ba^{2+} and Sr^{2+}, acetic acids, acetate ion, bisulphate ion and sulphate ions [9–11]. The mechanisms of sweet and sour corrosion and corrosion mitigation measures in oil and gas environments are described in Sections 4.1 – 4.3.

4.1. Sour corrosion

Sour corrosion occurs in environments with high concentration of hydrogen sulphide combining with water from oil and gas reserves [2,70–73]. Initially reported in Louisiana and Texas oil wells during the 1940 s, sour corrosion or sulphide stress cracking (SSC) has been a longstanding problem in the oil and gas industry. Based on the National Association of Corrosion Engineers (NACE), a sour corrosion environment is a function of the type of crude, operating conditions and the concentration and partial pressure of H_2S as given in Fig. 4 [74]. Based on the four main regions, factors contributing to sulphide stress cracking and sour corrosion can be ascertained. Within Region 0, there is no SSC and sour corrosion for pH $>$ 3.5. The area below pH of 3.5 is the threshold and where the pH of H_2S is relatively low. In case of Region 1, no SSC and sour corrosion was observed for low H_2S partial pressures and high pH. The transition zone is Region 2 which requires the domain knowledge and critical metallurgical parameters. This requires the need for the right material as it is an intermediate domain which is affected by a slight change in the H_2S partial pressure. Region 3 is the domain for SCC hence the need for corrosion resistant alloys. To ascertain the dominant corrosion phenomenon in H_2S/CO_2 system, when the ratio of CO_2 partial pressure to H_2S partial pressure is less than 20 then H_2S corrosion is dominant. However, if the pCO_2/pH_2S is greater than 500, then CO_2 corrosion is prevalent. The presence of H_2S can enhance CO_2 corrosion. An environment with $20 \leq pCO_2/pH_2S \leq 500$ exhibits mixed corrosion accelerating anodic dissolution through sulphide adsorption or suppression of CO_2 corrosion by virtue of protective sulphide scale formation.

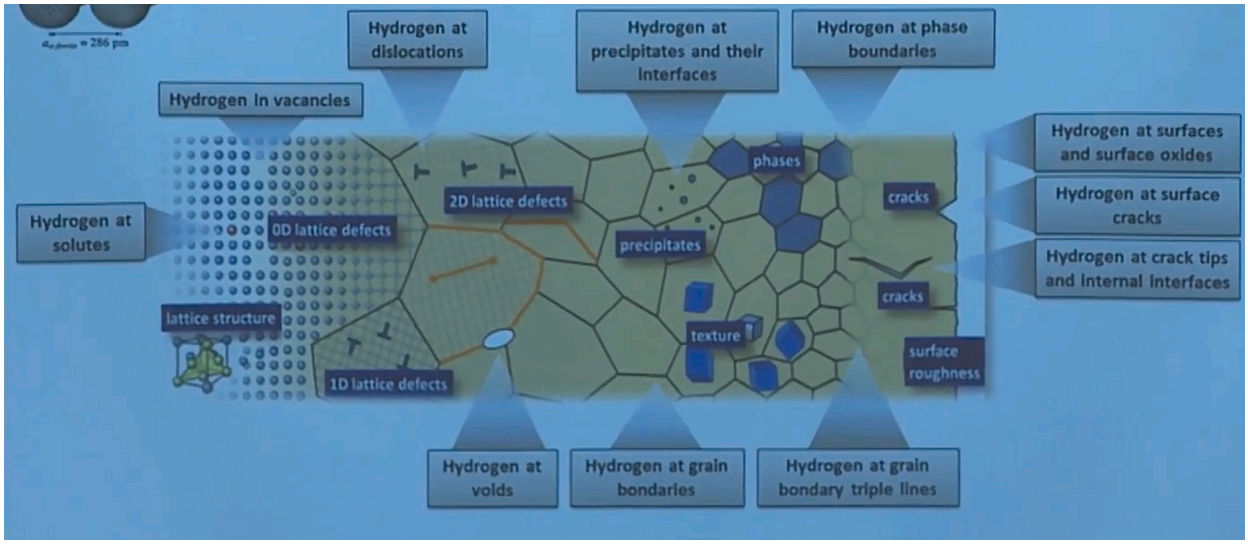

Fig. 5. Schematics showing the effect of hydrogen on various microstructural defect length scale in an alloyed material [13].

4.1.1. Effect of hydrogen sulphide environment

The H_2S is an extremely aggressive, highly toxic gas and common in oil and gas reserves accelerating the metal dissolution rates [9,50,73–75,78]. The main mechanisms causing sour corrosion include: (i) sulphide stress cracking which is as a result of H_2S penetrating the surfaces of the metallic component. This allows the diffusion of hydrogen atoms into defect sites in the metal lattice. This results in embrittlement which further leads to cracks under the application of stresses, (ii) the H_2S easily reacts with moisture in the environment to form sulphurous and sulphuric acids. These acids have pH below 4 and are aggressive environment for the initiating of corrosion phenomena increasing the rate of the metal dissolution at the anode (Fig. 4) [74].

The choice of materials used in sour environments is highly influenced by the presence of H_2S.The mechanism for sour corrosion is driven by galvanic coupling between Pyrite (FeS_2) and iron by the electrolytic cell, $Fe_{(s)} \mid Fe^{2+}_{(aq)} \parallel FeS_{2(s)} \mid FeS_{(1\text{-}x)(s)}$. The anodic reaction is the oxidation of iron, whereas the cathodic reaction is Pyrite reduction to iron sulphide, according to Equations (1) and (2) [74]. The process is generally accompanied by H_2 evolution, which is cathodic in nature. This can lead to severe hydrogen embrittlement in most low carbon steels. Although, not the subject of discussion, hydrogen atoms in metallic components can cause serious embrittlement challenges. The severity of hydrogen atoms are schematically shown in Fig. 5 [13].

$$Fe \rightleftharpoons Fe^{2+}{}_{(aq)} + 2e^{-} \tag{1}$$

$$Fe + H_2S \rightarrow FeS + H_2 \tag{2}$$

Major causes of corrosion-related accidents in the petroleum industry with 53 incidents involving sulphur compounds, water and hydrogen sulphide across the European Union is reviewed [50]. Hydrogen absorption into the metal lattice is the major cause of sour corrosion [19]. Other factors known to synergistically work with hydrogen sulphide to induce the renowned failure mode associated with sour corrosion include sulphides, H_2S, HS, and S_2 absorbed on the metal [19,75–67], solution acidity [2,77–67], elevated temperature and presence of CO_2. Sour corrosion can result in both localized and uniform corrosion.

4.1.2. Effect of hydrogen on the SSC process

Hydrogen ingress in structural metals is the predominant mechanism in SSC [79–85]. Hydrogen attack on many microstructural features and defects are dire as shown in Fig. 4 [73,74]. Hydrogen in structural metals causes loss of ductility and increased fracture stress, a phenomenon known as hydrogen embrittlement [86–88]. The severity is due to the ease at which hydrogen attack is fast and quick with adverse effects on the physical, chemical and mechanical behaviour of structural metals [13]. Generally, structural metals adversely affected by HE include stainless steels (austenitic, ferritic and martensitic), Ti alloys, Al alloys, Ni alloys and other forms of structural steels [73,86,89–92]. Considering structural steels accounting for ~ 70 % of structural applications, the effects of HE are

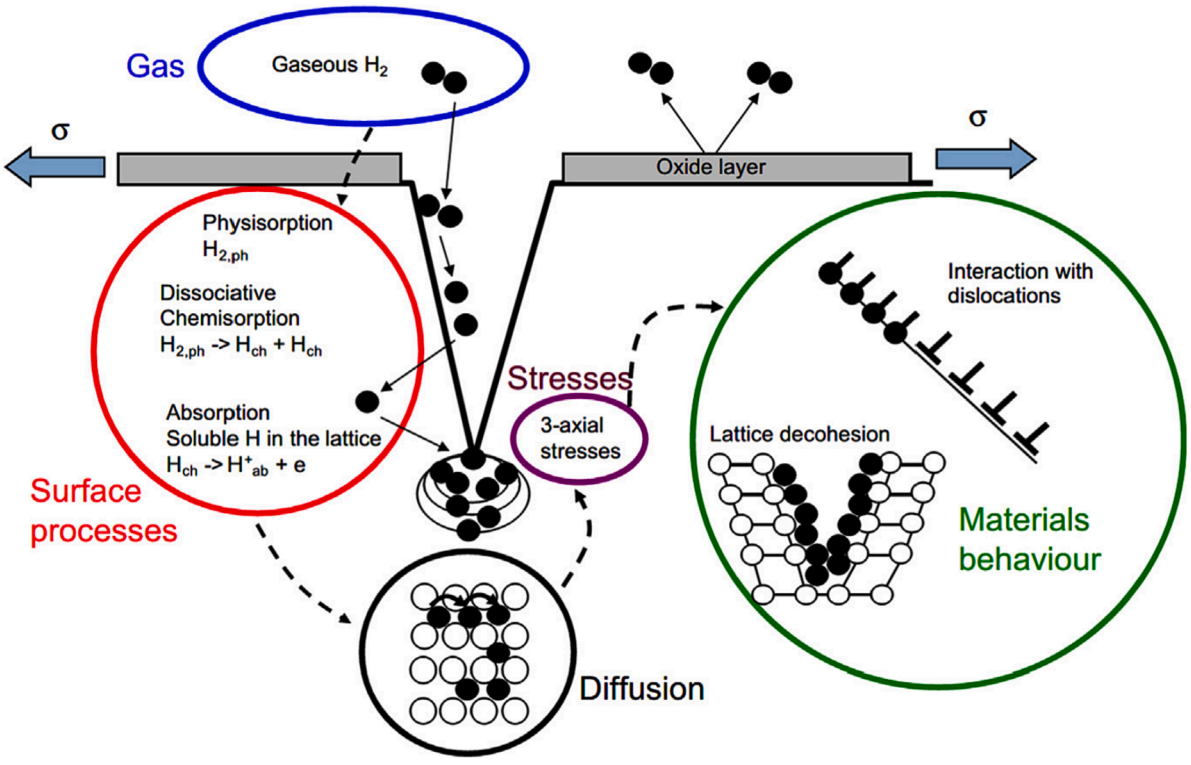

Fig. 6. Hydrogen interaction mechanisms with corrosion resistance alloys [56].

prominent precursor to other forms of failure and metal degradation [13].

The severe nature of SSC has led to failure of mechanical systems in the oil and gas industry [71–73]. The high amount of hydrogen sulphide gases in HTHP oil and gas wells are the precursor for the occurrence of SSC. The high temperatures and high pressures are harsh and aggressive conditions that facilitate the corrosion of mechanical components or structures with the combining devastating effects of H_2S gases. The mechanisms of SSC comprised of tensile stress, the H_2S and the mechanical component. Generally, hydrogen atoms from the H_2S diffuse into the pipe vessel attacking the microstructural features and defects. This is schematically showed in Fig. 5 [13], whereas the diffusion mechanisms causing hydrogen induced cracking is given in Fig. 6 [56].

The hydrogen atoms from the H_2S environment contributes to the hydrogen induced cracking [56,60,62,63]. This is a kind of hydrogen assisted cracking mode with no load effect. The main mechanism is diffusion of the hydrogen to the surface of the steel pipes transporting the crude oil. The various interaction stages of hydrogen with most conventional alloys within the HPHT domain is given in Fig. 6 [56]. Irrespective of the source of hydrogen atoms around the steel pipes, diffusion is inevitable and occurs in three distinct stages [56–63]. The first is the physisorption process where secondary and weak van der Waal interaction forces are generated between the surface of the pipe and the adsorbent atom. At this stage, the hydrogen atoms and the pH of the system are driving forces. The next stage is the dissociative chemisorption where the atoms at the surface and that of the absorbent undergoes a dissociative chemical reaction. This then gives way to the final stage where there is absorption, where the soluble H ions enter the lattice of the metal [13,56,58,60,62]. At each stage there is an interaction with dislocations and lattice decohesion with associated stress and strain fields [56–58,60].

4.1.3. Effects of other essential factors to sour corrosion mechanisms

Temperature and flow rate contributes to the rate of materials dissolution under sour corrosion. Although, overall effects of temperature is difficult to quantify, it does contribute to the sour corrosion mechanism. The temperature gradient is critical as it causes disturbance in chemical transfer reaction, the charge, the rate of solubility and how the surface layer is formed. The initial corrosion rate of the system increases with increasing temperature. However, after sometime, due to the formation and transformation of mackinawite, the effect of temperature decreases.

Flow rate contributes to overall sour corrosion rate at low H_2S partial pressure. The flow rate is proportional to the corrosion rate. The velocity of the crude in the pipe initially increase the rate of corrosion but its effects reduces drastically as the corrosion process continue over time. In case of pitting, high flow velocity is detriment as minutes cavities and defects are easily formed.

4.2. Sweet corrosion

Sweet corrosion, also known as CO_2 corrosion, occurs in the oil and gas industry [5–8]. These are mainly in natural gas and oil reservoirs [70]. The CO_2 environment accelerates the metal dissolution rate in the aqueous media by increasing rate of hydrogen evolution [16,93,65]. The carbon dioxide dissolves in water to form H_2CO_3, the main corrosive agent. Although H_2CO_3 is a weak acid, it reacts with Fe, main constituent element in structural steel infrastructure to form Fe^{2+} and bicarbonate ions [9–12,94]. The corrosion process involves both cathodic and anodic reactions with CO_2 accelerating the kinetics of cathodic reactions, which causes the rate of corrosion to rise [95]. The presence of bicarbonates in the phase raises the alkalinity of the fluid, which in turn lowers the corrosivity of the environment. In the absence of oxygen, the reactions that lead to the production of sweet corrosion are presented in Equations (3) and (4) [96–99]. The reduction of protons is supplied by the carbonic acid, at the cathodic sites on the metal surface. The reduction of protons leads to the formation of hydrogen gas contributing to the overall corrosion process. The hydrogen gas generated (Equation (4) can lead to localised corrosion and the formation of hydrogen bubbles on the metal surface. The CO_2 corrosion can be accelerated in the presence of oxygen and organic acids. Oxygen and organic acids destroy the protective iron carbide and carbonate (siderite ($FeCO_3$)) scales, inhibiting further scale development [9,12,94]. Oxygen is easily reduced in the presence of water to form hydroxides and enhances the alkalization of the local environment to drive the corrosion mechanism.

Anodic reaction:

$$Fe \rightleftharpoons Fe^{2+} + 2e^- \tag{3}$$

Cathodic reaction:

$$2H^+_{(aq)} + 2e^- \rightleftharpoons H_{2(g)} \tag{4}$$

The widely accepted mechanism for sweet corrosion is discussed briefly [9–12,94]. The first step involves establishing equilibrium between CO_2 in the gas and aqueous phase (Equation (5). After dissolving the CO_2 in water, the weak carbonic acid (H_2CO_3) is produced (Equation (6). Furthermore, the H_2CO_3 dissociates in two steps depending on the pH, releasing H^+ and bicarbonate (Equation (7) or tricarbonate (IV) (Equation (8). At pH < 4, hydrogen could evolve by the recombination of H^+ ions as shown in Equation (9). The reaction between the carbonate ions (Equation (8) and the free Fe^{2+} from the dissolution of steel that leads to initial dissolution. However, after sometimes, the corrosion products on the surface of the steel adheres acting as passive film that slows that the rate of metal dissolution. The protective layer is formed by the slow precipitation of solid $FeCO_3$(s) on the steel surface as $FeCO_3$(aq) [100–103]. This accumulates at the steel/solution interface until a saturation limit is reached. Significant contributions to the formation of $FeCO_3$(s) are water chemistry, temperature, pH, and CO_2 partial pressure. An equation representing generalized CO_2 corrosion of carbon steel is shown in Equation (11) [16,104,105].

$$CO_{2(g)} \rightleftharpoons CO_{2(aq)} \quad (5)$$

$$CO_{2(aq)} + H_2O_{(l)} \rightleftharpoons H_2CO_{3(aq)} \quad (6)$$

$$H_2CO_{3(aq)} + e^- \rightarrow H^+{}_{(aq)} + HCO_3{}^-{}_{(aq)} \left(pH = 4-6\right) \quad (7)$$

$$HCO_3{}^-{}_{(aq)} + e^- \rightarrow H^+{}_{(aq)} + CO_3{}^{2-}{}_{(aq)} \left(pH \geq 6\right) \quad (8)$$

$$2H^+{}_{(aq)} + 2e^- \rightleftharpoons H_{2(g)} \left(pH < 4\right) \quad (9)$$

$$Fe^{2+} + CO_3{}^{2-}{}_{(aq)} \rightarrow FeCO_{3(s)} \quad (10)$$

$$Fe_{(s)} + CO_{2(aq)} + H_2O_{(l)} \rightleftharpoons FeCO_{3(s)} + H_{2(g)} \quad (11)$$

Generally, $FeCO_3$ can be formed at low temperatures (typically below 90 °C) under high pH conditions [100,101]. However, the precursor species include $Fe_2(OH)_2CO_3$, $Fe_6(OH)_{12}CO_3{\cdot}H_2O$, $Fe_6(OH)_{12}CO_3$ and $Fe_2O_2CO_3$ [100,101]. These carbonate species can be transformed into protective $FeCO_3$ layers as the temperature increases. The sweet corrosion resistance of steel is more closely related to the morphology of $FeCO_3$ than to its formation. The $FeCO_3$ layer is more protective at elevated temperature than at low temperature. Scale growth of $FeCO_3$ occurs slowly and temperature-dependently [100,101,106]. This clearly shows the importance of temperature in the evolution of $FeCO_3$ layer with a protective morphology. Nucleation and growth of $FeCO_3$ grains are facilitated by higher temperatures, which are key factors controlling the formation of rhombohedra crystals. Even so, $FeCO_3$ adhesion is also influenced by the microstructure of the steel substrate beneath [13]. For detailed literature, systematic reviews, and currently published work on sour and sweet corrosions with associated mechanisms, some suggested references are presented [5–9,12,27,88,107–116].

5. Corrosion mitigation measures

Corrosion is the major known challenge in oil and gas industry [54,67,70,117]. However, corrosion control and prevention has been a major factor in curbing its devastating effects in the Oil and Gas Industry [67,70]. The selection of appropriate corrosion resistant material [36,19,67,70,117,3], the use of inhibitors [17,70,118,77], coatings [119,120] and cathodic protection [65] among

Table 2
Nominal compositions of conventional alloys for Oil and gas applications without trace elements [2].

Alloy and commercial name	Standard nominal composition (wt%)							Yield strength (MPa)
	Cr	Mo	Ni	C	Si	Mn	Fe	
Carbon and low alloy steel grades								
API 5L-X65Q (PSL 2)	–	–	–	0.2 max	0.5 max	1.7 max	Bal	450
ASTM A694 F65	–	–	–	0.3	0.2 – 0.3	1.6		
ASTM A 508 Grade 4	1.5 – 2.0	0.4 – 0.6	2.8 – 3.9	0.23	0.4	0.2 – 0.4		690
UNS K32047	1.5 – 1.9	0.5 – 0.7	3.0 – 3.5	0.1 – 0.2	0.2 – 0.4	0.2 max		
UNS K21590	2.0 – 2.5	0.9 – 1.1	0.25	0.1 – 0.2	0.10	0.3 – 0.6		517—586
UNS G43200	0.4 – 0.6	0.2 – 0.3	1.7 – 2.0	0.2 max	0.2 – 0.4	0.5 – 0.7		414
10GN2MFA	0.3	0.4 – 0.7	1.8 – 2.3	0.12 max	0.2 – 0.4	0.2 max		
Precipitation-hardened low alloy steels								
ASTM A 707 – L5	0.6 – 0.9	0.2 – 0.3	0.7 – 1.0	0.07 max	0.4 max	0.1 max		517
Solution annealed Ni-based alloys								
UNS N06625	20 – 23	8 – 10	58 min	0.1 max	0.5	0.5	5.0	290—414
Austenitic stainless steels								
UNS 31,603	16 – 18	2 – 3	10 – 14	0.03 max	1.0 max	2.0	Bal	182
UNS S31254	19 – 21	6 – 7	18 – 20	0.02 max	0.8 max	1.0 max	Bal	310
Martensitic stainless steels								
UNS S41000	12 – 14	–	–	0.15 max	1.0 max	1.0 max	Bal	550
UNS S17400	15 – 18	–	3 – 5	0.07 max	1.0 max	1.0	Bal	724
Duplex stainless steels								
UNS S32205	21—23	2.5 – 3.5	4.5 – 6.5	0.03 max	0.7 max	2.0	Bal	450
UNS S32750	24—26	3 – 5	6 – 8	0.03 max	0.8 max	1.2 max	Bal	550
UNS S32760	24 – 26	3 – 4	6 – 8	0.03 max	1.0 max	1.0 max	Bal	
UNS S39274	24 – 26	2.5 – 3.5	6 – 8	0.03 max	0.8 max	1.0 max	Bal	
Precipitation-hardened Ni-based alloys								
UNS N07718	17—21	2.8 – 3.3	50 – 55	0.045	0.01 max	0.35 max	Bal	827—968
UNS N07725	19 – 23	7 – 10	55 – 59	0.03 max	0.2 max	0.35 max	Bal	~827
UNS N07716	19 – 22	7 – 10	59—63	0.03 max	0.2 max	0.20 max	Bal	827—965
UNS N06059	22 – 24	15 – 17	Bal	–	0.10 max	0.5 max	1.5 max	450
UNS N06080	21	7	Bal	0.01 max	–	–	0.1 max	550—665
UNS N06686	19 – 23	15 – 17	Bal	0.01 max	0.08 max	0.75 max	5.0 max	760

others are successful and popular corrosion control mechanisms. The oil and gas industry make use of a wide variety of materials resistant to corrosion, including metals and non-metals [9–12,54]. When it is observed that the materials currently being used are susceptible to corrosive attack, it is usually decided to change the materials of construction and select alternative materials that are more suited to meet the specific demand [66]. Many different grades of stainless steel are utilised in oil and gas applications; the grade chosen is determined by the specific requirements of the operating environment. Stainless steels cover a wide range of alloys, each with a combination of corrosion resistance and mechanical properties. Suggested corrosion-resistant alloys for the oil and gas industry include 13Cr, S13Cr, 22Cr duplex, 25Cr duplex, 28Cr stainless steel, 825 nickel alloy, 625 nickel alloy, 2550 nickel alloy, and C276 nickel alloy [54,121]. Other classes of CRAs used in the oil and gas industry are martensitic stainless steels, martensitic–ferritic stainless, austenitic-ferritic duplex, Ni-Fe-Cr alloy, Ni-Fe-Cr-Mo alloys, Ni-Cr-Mo alloys, precipitation hardenable alloys, and other nickel alloys (Table 2) [3].

Inhibitors are another type of corrosion mitigation strategy, and they are composed of compounds that are used to protect the surface of metals used in the oil and gas sectors against corrosion [17,18,118,122–124]. In the oil and gas industry, corrosion inhibitors are often only effective in preventing sweet and sour corrosion [125,126]. Consequently, inhibitors are necessary to prevent several types of corrosion, including general, under-deposit, galvanic, top-of-line, and preferential weld corrosion [65,125–127]. A corrosion inhibitor can slow down either the anodic process or the cathodic process by merely blocking active spots on the surface of the metal [128]. Inhibitors can be categorised as water-soluble, oil-soluble, or both oil-soluble and water soluble [125,126]. Inhibitors that can be used in the oil and gas industry include 3-phenyl-2-propyn-1-ol, dibenzylidene acetone, propargyl, cinnamaldehyde, methyloxyphenol and nonylphenol, carboxylic acid and aldehydes, amines, chromates, nitrites, molybdates, polyphosphates, phosphonates, imidazoline, mercaptobenzothiazole, benzotriazole, and tolyltriazole.

Many factors influence inhibitor selection and these are becoming prevalent as oil and gas are developed from fields that have increasingly severe conditions. Some of these factors include identifying the problem that needs to be solved, identifying the corrosive species, the availability of the inhibitor, the cost of the inhibitor, the environmental friendliness, the pressure and temperature, velocity, toxicity, production composition, water/oil ratio, the salinity of the water, and the acidity of both the water and the oil [65,128,129]. Corrosion inhibitor effectiveness can be affected by several physical conditions such as salinity, pH, temperature, and gas/liquid velocity [128,125]. To address the performance of corrosion inhibitors, important performance indicators were developed. These indicators are as follows: corrosion rate (less than 4 mpy and no localised corrosion); corrosion inhibitor residual (more than 75 % partitioning); corrosion inhibitor availability (more than 95 %); overboard oil-in-water quality (less than 30 mg/L); and corrosion inhibitor dose rate (less than 10 %) [125]. Therefore, when choosing a corrosion inhibitor, it is essential to determine the type of corrosion that occurs in the field. Furthermore, tests that are meant to evaluate the effectiveness of the inhibitor need to be carried out in conjunction with the key performance indicators to prevent the form or forms of corrosion that are present. A combination of cathodic protection and coatings is the most effective strategy for minimising the effects of external corrosion on buried pipelines. Protective coatings are another corrosion mitigation method that is commonly used in the oil and gas sectors.

A protective coating layer or barrier on the material to avoid the direct contact with the process media will enhance the material and equipment life. The barrier layer may be comprised of paint, a coating, or a lining; a metallic lining; metallic sheets; or cladding [20]. There are also non-metallic linings such as fibre glass, glass flake, epoxy, and rubber that are typically carried out on the equipment such as separators, knock-out drums, and storage tanks [65]. New coatings made of non-metallic materials like graphene and 2D materials are now being explored for a variety of uses, and these coatings have the potential to integrate molecules that limit corrosion into their matrix [64]. When the protective film is damaged, the molecules that inhibit corrosion become activated, which enables them to spontaneously guard the exposed metal surfaces. The Fusion-bonded epoxy (FBE) and three-layer polyolefin (3LPO) (polyethylene or polypropylene (PP)) coating systems are currently the most extensively used external anti-corrosion coating systems [65]. It is essential to have a consistent protective coating that can withstand the increasingly harsh conditions that are present in oil and gas pipelines.

The process of cathodic protection involves sending a current to the pipeline through the soil from an external source. This current then overrides the local anodes, turning the entire exposed pipeline surface cathodic [130]. This is achieved by moving the potential of the metal surface in the negative direction by using an external current source. Cathodic protection is applied using sacrificial anodes such as magnesium, zinc, and aluminium when the protective current required is less than 4 to 5 A and the resistivity of the electrolyte (or environment) is typically below 10,000 O-cm [130]. The sacrificial metal corrodes; hence, the application of cathodic protection does not remove corrosion; rather, it transfers it from the structure that is important to another metal that is less important. When only the coating is applied without cathodic protection, the likelihood of localised corrosion occurring in those areas where the coating fails is increased [119,120]. Therefore, coating, and cathodic protection work together. The efficiency of cathodic protection is determined by several factors, including protective coatings, maintenance capacity, environment, temperature, stray currents, and DC stray current [130]. The next section highlights the associated corrosion related challenges and justifies CCAs as a potential material in oil and gas high HPHT fields.

6. Current material challenges in the oilfield environment

There are about five major material challenges associated with most high pressure and high temperature systems. These include aggressive corrosion, thermal degradation, excessive pressures causing erosive wear and cyclic stresses leading to mechanical fatigue. To increase material life cycle of mechanical components for HPHT applications, mechanical considerations, manufacturing capabilities, metallurgical perspectives and corrosion resistance of the applied materials need to be addressed. Corrosion resistant alloys such as Ni-based and stainless steels are used to reduce the severity of corrosion. In case of thermal degradation, the effects are due to

high temperatures reducing the structural strength and increasing the susceptibility to failure. Thus, heat resistant materials such as refractory metals and some ceramics are designed and used under HPHT conditions. Over time, cyclic stresses and strains experienced in HPHT wells lead to fatigue failures, which is time dependent deformation mechanism. Thus, fatigue resistant alloys are generally used to improved useful fatigue lives.

About 90 % of materials used in oil and gas fields are made from carbon and low alloy steels (LAS) due to the balance of cost and mechanical properties [9–12,18,94,101–103,131]. Despite the structural advantages of carbon steels and LAS, they are highly susceptible to uniform and localised corrosion in HTHP environments [19,132]. Thus, a transition from LAS to corrosion resistant alloys (CRA) is desirable for crude in unproven reserves [3]. Corrosion resistant alloys has higher alloying elements (Cr, Ni, Mo, Al, Co, Nb, Cu, Ti) than in LAS with associated passive oxides film, a barrier between the reactive ions and the well materials [14,3,132–134]. Stainless steels are one of the main corrosion resistant alloys with a minimum amount of Cr being 10.5 wt%. While Cr increases the corrosion resistance of iron [135], Ni and Mo stabilizes the passive film [136–138 139].

The benefits of Mo to corrosion resistance are empirical. However, the underlying mechanisms are still lacking [112,140–144]. Two main arguments have been advanced to support the role of Mo in corrosion resistant alloys. The first is the stabilization of the passive film, which is attributed to compositional change of the passive film induced by Mo addition as observed in some corrosion resistant alloys [112,140–143]. This enhances the kinetics associated with localised corrosion by decreasing the active dissolution rate making it difficult for continuous localized corrosion to occur [140,145–148]. Traces of Mo have been observed in the passive films of Fe-Cr-Mo alloys upon dissolution resulting in reduced dissolution current density [145,149]. Similarly, the effects and traces of Mo on the pitting resistance under alkaline conditions have also been reported [140,141,148,149]. Generally, the passive film enhancement of Mo is pronounced on ferritic and duplex stainless steels [107,150]. However, this is largely inconclusive for austenitic stainless steels [151,152]. Molybdenum in corrosion resistant alloys impedes the dissolution kinetics [107–111,150,153–155]. This shows similar features as the addition of molybdate inhibitor in the corrosion media. During the initiation process of localised corrosion, Mo dissolves forming insoluble molybdate ions with clouds of cationic species in the solution. This reduces the metal ion concentration in solution, thus reducing the severity and aggressive actions of the anionic species such as chlorides and sulphates in the solution. The corrosion current density is then reduced which hinders the localized corrosion rate making it easy for new nucleation sites to repassivate. The molybdate ions also reacts with OH and H ions in solution to form MoO_2 thus decreasing the concentration of OH and H ions thereby reducing the aggressiveness of the solution [156]. Generally, the corrosion resistance of the alloy is driven by cocktail effects of the constituent elements and its effects on interfacial oxides and films. Common ways of improving the corrosion resistance of stainless steels have been explored through cold rolling, sputtering, and surface mechanical attrition treatment [157]. The grain size effects on corrosion resistance have been reported, although inconclusive.

Precipitation hardening Ni-based CRA materials have been used for aggressive and harsh corrosion environments [158,159]. They have high resistance to stress corrosion cracking. Nickel increases the stacking fault energy (SFE) resulting in desirable low planar slip, thus reducing the susceptibility to pitting corrosion. Nickel also increases stress corrosion cracking resistance [121,160]. The passive films on most CRAs are susceptible to localized corrosion under HPHT environments [133]. In chloride environments, Cl^- ions are adsorbed on the surface of the component, thus penetrating the oxide films rapidly at elevated temperatures [161]. Most cases studied on corrosion failure in oil and gas originated in pipe works, causing 71 % of the accidents studied [162]. In August 2012, leakage due to sour corrosion resulted in a ~$50 million loss to a petroleum refining industry in France. According to the report only one life was lost on the day of the accident along with other significant injuries to workers. About 15,000 residents of the towns nearby requested medical care a week later due to breathing ailments. In Colombia, in December 2012, a report suggested that about 76 million cubic feet of natural gas equivalent to $285,000 was released and burned following a rupture caused by localized corrosion. Even though lives were not lost in this accident, close to $9 million was lost [163].

The catastrophe and cost associated with sour and sweet corrosion have led to increased research into materials to mitigate it. For HPHT environments which are more aggressive, alternative materials with superior corrosion resistance should be considered. This would increase structural integrity, prevent sudden failures, and reduce downtime due to unplanned plant shutdowns to save cost. Due to the elevated temperatures (above 130 °C) and high pressures (13 atm), the use of conventional alloys is problematic [121]. The CCAs have shown better properties than most of the austenitic stainless steels currently being used in proven reserves where the corrosion environment is less aggressive than in HPHT wells [164–166]. The next section highlights the properties of complex concentrated alloys as potential materials in the oil and gas environment.

7. Complex concentrated alloys for oilfields

Complex concentrated alloys are based on multiple principal elements with compositions in near equal amounts. This concept relies on alloy-by-design approach within the domain of rational alloy design for structural and functional applications. These alloys extend the frontiers for alloy design beyond conventional alloys [164–169]. The wide compositional space offers potential for property combinations (mechanical and corrosion properties) out-performing conventional alloys. Most CCAs are more tolerant of compositional variation which is critical for tailoring compositions and microstructures for the desired application. This alloy design strategy is expected to close the niche areas around multi-principal element alloys that have been neglected due to the initial complexities of forming intermetallics and detrimental precipitates. The microstructures of CCAs are single-phase, metastable phases and multiple phases with varying concentrations of constituents ranging 5——35 at%. Currently, non-equal compositions of constituent elements are also being explored to reduce cost [168]. The great properties (mechanical, physical, corrosion and functional) are attributed to the four core effects [170]. These effects are high entropy stabilization of the phase which drives the thermodynamics, sluggish diffusion which speaks to the kinetics, severe lattice distortions influencing crystal structure and metallic cocktail resulting in property

improvement [171]. Detailed understanding of these core effects and debates around their overall contribution to elucidating CCAs are reviewed [164–166,168–170,172–167]. There is the bone of contention regarding the overarching roles of the four core effects to the physical metallurgy of CCAs. A timeline focusing on various microstructural pathways and its effects on property assessment and evaluation is given in Fig. 7 [174]. These microstructural features are tailored to drive the relevant structural and functional properties.

These alloys are very promising with cornucopia of structural and functional properties [166,175]. Most of the properties of yet to be optimized compositions of bulk CCAs compared favourably with conventional dilute alloys. The CCAs are heavily alloyed materials and have corrosion and oxidation resistant alloying elements much higher than stainless steels and Ti-based alloys [15,176]. The multiple and metastable phases have been explored for enhanced mechanical, corrosion and oxidation resistance [177–181]. Some of the 3D transition CCAs and their corrosion behaviour and possible applications in harsh environments such as high pressure high temperature wells are discussed.

7.1. Bulk CCA alloys and their corrosion behaviour

The environmental behaviour (corrosion and oxidation resistance) of CCAs is influenced by the composition, processing conditions and microstructural features (Fig. 8) [182]. In most instances, another contributing factor is the nature and morphology of the passive film formed. From compositional standpoint, it is either equal or non-equal proportions of constituent elements. These alloying elements are carefully selected and measured to induce the right properties, i.e., corrosion resistance. Considering the corrosion resistant alloying elements are higher than conventional stainless steels, superior corrosion resistance at ambient temperatures and high temperature oxidation resistance are achievable [32,183–185]. Some of the main alloying elements affecting corrosion resistance have been reported [32,183–185]. These elements are Cr [32], Ni [32,184], Ti [15], Mo [186–188]. These elements provide the cocktail effects critical for CCAs.

Generally, interstitial CCAs are currently being studied for corrosion resistant and other functional applications [87,189–193]. Such elements are C, N, O, Si and B with simultaneous effects of mechanical and corrosion resistance [194–200]. The general and pitting corrosion behaviour of some CCAs have been studied and compared with some of the corrosion resistant alloys [23,37,201–203]. Better corrosion resistance of CCAs than stainless steels is attributed to the cocktail effects of the constituent elements [32,33,204]–[157]. Based on the principal of configurational entropy, stainless steels, which are corrosion resistant alloys fall under medium entropy alloys, with the entropy of mixing ranging from 0.96R to 1.15R J/Kmol (where R is the real gas constant, value = 8.314 J/Kmol) [201,203]. With high entropy alloys of Cr, Mo, and Ni above 15 at%, the corrosion resistance of CCAs is improved. For instance, the pitting potential of Cu0.5NiAlCoCrFeSi alloy was lower in 0.1 to 1 M NaCl solution than in 304 austenitic stainless steel grade [207]. Thus, the CCA had high resistance to pitting corrosion, and the effects are driven primarily by Cr content [208].

The corrosion resistance of over 20 CCAs was significantly higher than most carbon steels and Al alloys. The corrosion resistance of Cr, Co and Ni-containing CCAs showed improved corrosion resistance than most stainless steels. Thus, the E_{pit}, E_{corr} and I_{corr} were dependent on the constituent elements of the CCAs [33]. Similarly, the corrosion behaviour of pure Ni, NiCo, NiCoCr, NiCoFe and

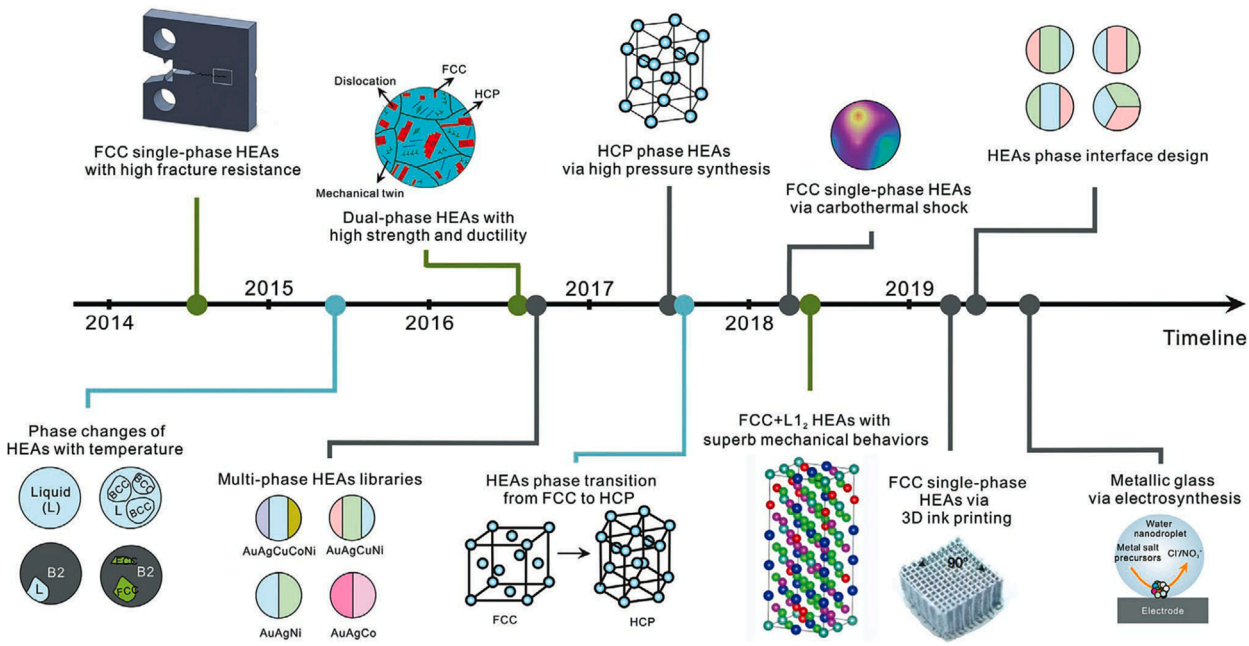

Fig. 7. Timelines for the microstructural pathways and property enhancement of high entropy alloys [174].

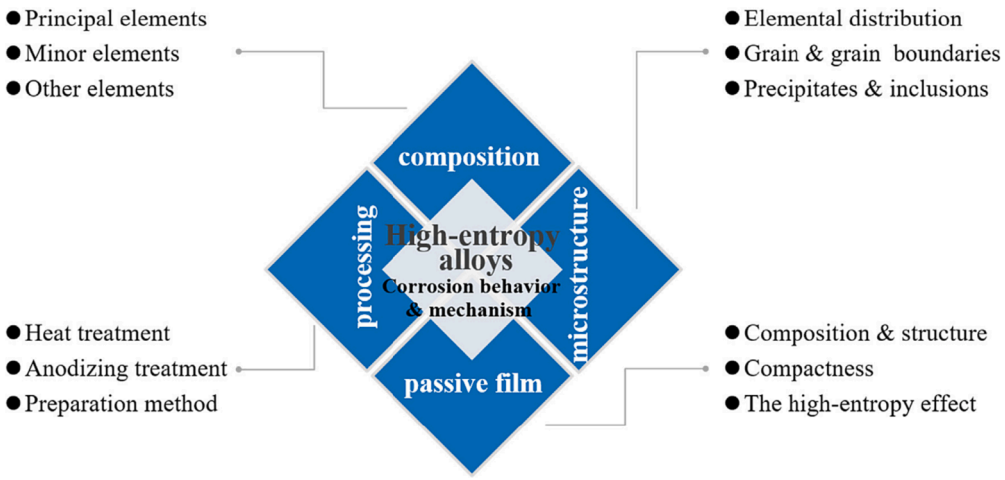

Fig. 8. Corrosion and environmental resistance based on composition-processing-microstructure-passive film formation of HEAs/CCAs [182].

NiCoCrFe in 0.1 M HCl and 0.1 M NaCl solutions have been studied [209]. All the alloys had the FCC solid solution. Cobalt addition to the pure Ni showed improved corrosion resistance and widened the passive potential region. The addition of Cr resulted in a further increase in corrosion resistance as expected. When Fe was added, there was a harmful effect on the corrosion of NiCoFe alloy. The pitting corrosion resistance of NiCoCrFe was further reduced. The trend for resistance to pitting corrosion is given as Ni < NiCo < NiCoFe < NiCoCrFe < NiCoCr [209]. The oxides and hydroxides of Ni and Fe in NiCoFe and NiCoCrFe alloys are porous and permeable and do not offer much protection during the electrochemical process. In chloride solution, reactive chloride ions increase the dissolution rate of the alloy by attacking the weak Ni and Fe oxides as opposed to the more stable and impenetrable Cr_2O_3. The latter improving uniform and pitting corrosion resistance.

Generally, iron oxides and hydroxides form porous passive films during the electrochemical reaction. The presence of Cl^- increases the dissolution rate by attacking ferociously the passive layer thereby exposing fresh alloy surface to further dissolution. On the contrary, the formation of the layer, was noticed to have improved the corrosion resistance of NiCoCr and NiCoCrFe considerably when Cr was introduced. For this reason, the 25 at % of NiCoCr and NiCoCrFe alloys contributed to the overall corrosion resistance. Similar

Table 3
Electrochemical characteristics of CCAs in various medium compared with some corrosion resistant alloys.

CCA systems	Corrosion medium	E_{corr} (mV_{SCE})	I_{corr} (A/cm^2)	General remarks	Refs.
$CuCr_2Fe_2Ni_2Mn_2$	1 M H_2SO_4	− 974	2.09 ' 10^{-6}	Increasing Cu content results in segregation of elements thus increasing corrosion rate	[210]
CrFeMnNi	0.5 M H_2SO_4	− 473	6.86 ' 10^{-4}	Corrosion rates were high with an active–passive transition especially in acidic media. Al has negative effect on corrosion properties	[215]
Al0.3CrFeMnNi	1 M NaCl	− 438	2.39 ' 10^{-3}		
Al0.5CrFeMnNi		− 450	5.08 ' 10^{-3}		
$Cu_{0.5}$CoCrFeNi	0.6 M NaCl	− 280	2.03 ' 10^{-9}	Poor corrosion resistance compared to 304L in the as cast and aged condition	[217]
AlCrFeMnNi	15 % H_2SO_4	–	–	Alloy anodized in the acidic medium	[218]
	5 % NaOH	–	–	Improved corrosion resistance	
$Al_{0.5}$CoCrCuFeNi	1 M H_2SO_4	− 359	7.87 ' 10^{-4}	Excellent corrosion resistance than AISI 304	[219]
$FeCrNiCoB_x$	0.6 M NaCl	–	–		[220]
$Al_{0.5}$CoCrFeNi		− 570	1.7 ' 10^{-7}	Preferential attack of the chloride ions on the Al-Ni rich phase	[214]
AlCrFeNiCoCu	1 M NaCl	− 12	3.23 ' 10^{-9}	Great corrosion resistance compared to 304 SS	[221]
$FeCoNiCuSn_x$	5 % NaOH	− 1030	9.49 ' 10^{-5}	Great corrosion resistance than AISI 304	
CoCrCuFeNiNb	1 M / 6 M HCl	− 397	8.93 ' 10^{-5}		[222]
FeCoNiCr	0.6 M NaCl	− 260	3.15 ' 10^{-8}	Dissolution is preferential at the Cu-rich FCC and the FeCoNiCr had better corrosion resistance compared to AISI 304L	[35]
$FeCoNiCrCu_{0.5}$		− 290	7.23 ' 10^{-7}		
$FeCoNiCrCu_1$		− 330	1.32 ' 10^{-6}		

effects of corrosion resistance of the high Cr content in CuCrFeNiMn in 1 M H_2SO_4 at 25 °C have been reported [210].

Various characterization techniques are used to probe the mixed oxide layer formed on CCAs [206,211]. Metals that easily reacts to form an oxide (usually associated with the highest negative Gibbs free Energy) takes charge of the passivation process of a CCA. Efforts to predict the ease of formation of oxides have been attempted using the ΔG of the constituent elements [211]. However, the unoxidized form of the elements can contribute to superior corrosion resistance [206].

Aluminium is one of the elements significantly impacting the microstructure and properties of Al-based CCAs [212,213]. Aside stabilizing the BCC phase, Al contributes to lightweight, increases microhardness and easily forms intermetallic with Fe such as AlFe, Al_5Fe_2, $AlFe_3$ [214,215]. The effect of intermetallics induce lattice strains promoting the severe lattice distortion. Despite the positive effects of Al, it has low nobility relative to the other multi-elements in most CCAs. This contributes to increased material dissolution with adverse effect on corrosion resistance [216]. The effect of Al contents on passivation properties of as-cast $Al_xCoCrFeNi$ (x = 0, x = 0.25, x = 0.50, x = 1.0) in 0.5 M H_2SO_4 and chloride concentrations of 0.25 – 1 M showed well-defined passive region between 0 and 1.2 V_{SHE} [216]. The CoCrFeNi and $Al_{0.25}CoCrFeNi$ had an FCC microstructure, whereas the $Al_{0.5}CoCrFeNi$ and $Al_1CoCrFeNi$ had mixed phases of FCC + BCC and BCC + B2 respectively. Thus, with increasing Al content, significant change in the microstructure from FCC to BCC with remarkable effect of corrosion behaviour was observed [216]. The alloys with BCC + B2 microstructure showed the best passivation behaviours in H_2SO_4 with selective dissolution of the Al-Ni rich phase of the ordered BCC phase.

The effect of temperature on i_{pass} with varying Al content on AlxCoCrFeNi has been observed [216]. For $Al_xCoCrFeNi$, $x \geq 0.5$, there is a positive effect on localized corrosion in simulated HPHT environments. The Al passivates spontaneously to form a porous protective film when in contact with H_2SO_4. However, the passivity due to the constituent element led to higher E_{corr} and lower i_{pass}, i_{cri} and i_{corr} than 304 stainless steels [216]. Based on the Helmholtz layer model, increased Al caused the formation of a thick and dispersive oxide layer reflecting the higher i_{pass}. The increasing of Al content increased the susceptibility of the CCA to pitting corrosion, with CoCrFeNi exhibiting the best anti-pitting resistance, followed by 304 SS and the remaining CCA in increasing x values.

Some of the CCA systems tested under various acidic and basic environments are presented in Table 3. The effects of the various corrosion resistant alloying elements have also been highlighted. Similarly, Table 4 shows electrochemical characteristics of CCAs in different concentrations of NaCl solution, whereas that in various acidic environment in Table 5. The corrosion behaviour of these alloys showed promising trends and easily optimizable for applications in HTHP environment.

The effects of microstructure on hardness and corrosion resistance of as-cast $Al_{0.5}CoCrFeNi$ alloy is discussed [214]. The XRD analysis showed that the CCA had a simple, stable FCC phase. An additional characterization using the SEM (BEI) revealed the presence of FCC droplet-shaped phase (DSP) in the metal/alloy matrix identified by [214] as Al-Ni rich phase. Further illumination on the behaviour of $Al_{0.5}CoCrFeNi$ in 3.5 % NaCl solution at ambient temperature led to a potential polarization test that showed an E_{corr} value of −0.57 V_{SCE}, i_{corr} of 1.70×10^{-7} A/cm^2 and E_p of 0.13 V_{SCE} as compared to E_{corr} value of −0.084 V_{SHE}, i_{corr} value of 13.4 and E_p of 0.017 V_{SHE} [216] in 0.5 M H_2SO_4. This suggests that high resistance of $Al_{0.5}CoCrFeNi$ to pitting corrosion in high pH environments than for low pH. The effect of Cr on corrosion resistant of AlCoCrFeNi CCAs is largely dependent on other alloying elements such as Al with high affinity for oxygen [37,46,214]. The passive film as characterized by X-ray photoelectron spectroscopy (XPS) showed significant amounts of Al_2O_3 than the tenacious Cr_2O_3. Although, the passive Al_2O_3 film was thicker, it was porous and less tenacious to induce corrosion resistance. This shows the dependence of the corrosion resistance of the alloy on composition, the corrosion media, the composition of the passive film and its density [37,46].

The effect of scanning rate on the electrochemical corrosion behaviour is studied [225]. The effects of Al on the corrosion behaviour of $Al_xCoCrFeNi$ in 3.5 % NaCl with multi-phase structures (BCC and BCC2) for $Al_{0.5}CoCrFeNi$ alloy is discussed. The addition of Al stabilized the BCC phase with the transition from simple FCC solid solution rich in Fe and Cr at Al = 0.3 to intensified peaks of BCC + BCC2 (Al-Ni rich) in $Al_{0.7}CoCrFeNi$. Equally, [225] just as [216] attributed the enhanced corrosion resistance in the $Al_{0.3}CoCrFeNi$ to the single FCC crystal structure and the presence of stable oxides arising from the increased Cr content at reduced Al molar concentrations. At higher Al, susceptibility to localize corrosion increases confirming the reduced passive region from 1227 mV to 1114 mV (x = 0 to x = 0.5) by a similar work [215]. Even though free corrosion current increases at high Al contents, most CCAs were more

Table 4
Electrochemical characteristics of CCAs in 3.5 wt% NaCl solution.

CCA systems	Fabrication processes	Corrosion medium	Phases	E_{corr} (mV_{SCE})	I_{corr} (mA/cm^2)	Refs.
$Al_{0.1}CoCrFeNi$	IM + HIP	3.5 wt% NaCl	FCC	− 0.225	0.638	[223]
$Al_{0.3}CoCrFeNi$	MS			− 0.451	0.103	[224]
$Al_{0.3}CoCrFeNi$	AM			− 0.195	0.0835	[225]
$Al_{0.5}CoCrFeNi$				− 0.57	0.17	[214]
$Al_{0.5}CoCrFeNi$				− 0.225	0.252	[225]
$Al_{0.7}CoCrFeNi$				− 0.275	0.429	
AlCoCrFeNi	IM			− 0.185	5.70	[226]
AlCoCrFeNi	LSA		BCC	− 0.167	0.073	[227]
AlCoCrFeNi	AM			− 0.294	0.093	[228]
AlCoCrFeNi	AM + ESD			− 0.349	0.016	
AlCoCrFeNi	LSA		BCC + BCC	− 0.73	0.3	[229]
AlCoCrFeNiTi	LSA			− 0.203	0.073	
AlCoCrFeNi	DLF	0.6 M NaCl	BCC + FCC	− 0.24	0.089	[229]
AlCoCrFeTi	MA + SPS	3.5 wt% NaCl	FCC + BCC	− 0.217	1.475	[229]
AlCoCrCu	PM	1 M NaCl		− 0.012	0.003	[221]

Table 5
Electrochemical characteristics of CCAs in acidic media.

CCA systems	Fabrication processes	Corrosion medium	Phases	E_{corr} (mV_{SCE})	I_{corr} (mA/cm^2)	Refs.
$AlCoCrCu_{0.5}FeNiSi$	AM	1 M H_2SO_4	Amorphous + BCC	− 0.17	251	[207]
Al0.5CoCrCuFeNc	IM	1 N H_2SO_4	FCC	− 0.115	780	[230]
$Co_{1.5}CrFeNi_{1.5}Ti_{0.5}$	IM	0.5 M H_2SO_4	FCC	− 0.092	30	[231]
$Co_{1.5}CrFeNi_{1.5}Ti_{0.5}Mo_{0.1}$				− 0.071	78	
$Co_{1.5}CrFeNi_{1.5}Ti_{0.5}Mo_{0.8}$			FCC + s (Mo, Cr)	− 0.07	69	
AlCoCrFeNi	LC	0.05 M HCl	FCC + BCC	0.55	29.2	[232]
Al1.8CoCrFeNi	LC			0.673	7.6	
$CuCrFe_2Ni_2Mn_2$	AM	1 M H_2SO_4		− 0.90	40.2	
$CuCr_2Fe_2Ni_2Mn_2$	AM		FCC	− 0.73	2.1	[232]
AlCoCrCuFe	LC	0.5 M H_2SO_4	FCC + BCC	− 0.109	10.4	[34]
CoCrCuFeNi	PTAC	1 N HCl	FCC	− 0.235	9.0	[233]
CoCrCuFeNiNb			FCC + laves	− 0.305	10.0	[222]
$Al_{0.5}CoCrCu_{0.5}FeNi$	AM	0.5 M H_2SO_4	FCC	− 0.112	4.2	[234]
$Al_1CoCrCu_{0.5}FeNi$				− 0.22	50.9	
$Al_{1.5}CoCrCu_{0.5}FeNi$				− 0. 172	0.2	
AlCoCrFeNiTi0.5			BCC + FCC	− 0.1	20.6	[235]
(CoCrCuFeNi)95B5	PTAC	1 N HCl	FCC + s	− 0.219	13.7	[236]
Al5Cr32Fe35Ni22Ti6	AM	0.5 M H_2SO_4	BCC + FCC + Heusler	− 0.13	35.2	[237]
AlCoCuFeNi			FCC + A2/B2	− 0.058	8	[238]
AlCoCrCuFeNi			A2/B2 + FCC	− 0.075	5.1	
(CoCrFeNi)80B20		0.1 M H_2SO_4	Amorphous	−0.226	0.2	[239]
HfNbTaTiZr		11.5 M HNO_3	BCC	0.0682	0.2	[240]
CoCrFeMnNi	EL	1 M HCl	FCC	− 0.350	0.3	[241]

PTAC – Plasma Transferred Arc Cladding, AM – Arc Melting, EL – Electrolysis, LC – Laser Cladding, IM – Induction Melting, MS – Magnetic Sputtering, HIP – Hot Isostatic Pressing.

corrosion resistant than 304 SS. Increased scanning rates increase the i_{pass}.

The electrochemical properties of the six-component $FeCoNiCrCu_{0.5}Al_x$ (x = 0.5, 1.0,1.5) CCA has also been studied [234]. The electrochemical behaviour of the alloys was tested in 0.5 M H_2SO_4 and 0.5 M NaCl solution and compared with 321 austenitic stainless (Fig. 9) [234]. The effects of ageing temperature with varying Al concentration were elucidated. The effect of heat treatment on the phase transformation of the $FeCoNiCrCu_{0.5}Al_{0.5}$ was negligible as both as cast and heat-treated had simple FCC crystal structure. There was transformation from an intermediate BCC phase (as-cast $FeCoNiCrCu_{0.5}Al_1$) to a stable mixed FCC + BCC phase after heat treatment at 1100 °C for 4 hrs. Increasing the Al content stabilized the BCC phase and so at x = 1.5, the stable BCC crystal structure transforms to precipitated FCC inter-dendrites in a BCC dendritic structure [234]. The precipitate (inter-dendrite) was rich in Al-Ni and high fraction of Al reduced thermal stability. In the 0.5 M NaCl, the $FeCoNiCrCu_{0.5}Al_1$ had the worst corrosion resistance due to the high i_{corr}, attributable to the multiphase microstructure, which could induce galvanic reaction. This results in a cathode/ anode galvanic coupling hence increasing the dissolution rate. The presence of Cl^- also contributes to the continuous aggressive attack on the protective film. As compared to the behaviour of the as-cast CCAs in acidic environments, alloys behaved differently with a large passive region.

The metastable nature of the FCC precipitate in x = 1.5 CCA increases the corrosion rate making it the worst in both basic and acidic environments [234]. The $FeCoNiCrCu_{0.5}Al_1$ had the best resistance to electrochemical attack compared to 321 stainless steels with wider passive and lower i_{corr} in alkaline region [234]. The hardness increased with increasing volume fraction of Al in the as-cast

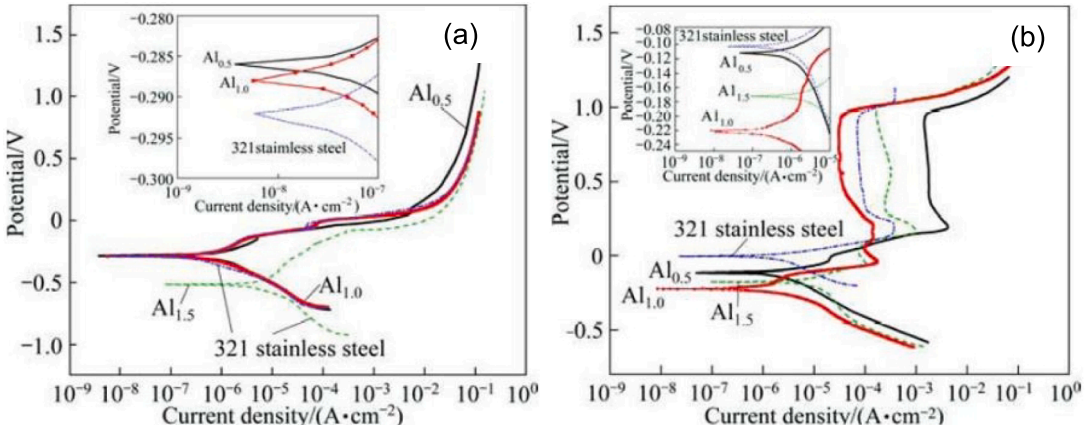

Fig. 9. Polarization curves for Al-based CCA and austenitic stainless steel grade 321 in (a) in 0.5 M NaCl and (f) 0.5 M H_2SO_4 [234].

condition, which is crucial property for a typical HPHT application. However, slight modification was observed for the hardness trends after the heat treatment process. The alloys with Al ≥ 1.0 at% showed low hardness after heat treatment due to the precipitated FCC phase which is low in hardness thus reducing the overall hardness of the BCC crystal structure. The $FeCoNiCrCu_{0.5}Al_{0.5}$ alloy showed an improved hardness after heat treatment.

The corrosion behaviour of single phase FCC $FeCoNiCrCu_x$ (x = 0, 0.5, 1) was studied in 3.5 % NaCl solution at ambient temperature [35,243]. Both $FeCoNiCrCu_{0.5}$ and $FeCoNiCrCu_1$ possessed dendrites and Cu-rich inter-dendrites. The FeCoNiCr showed the best resistance to pitting corrosion following the immersion test conducted on all the CCAs in 3.5 % NaCl solution at 25 ℃ for 30 days [35,243]. For pitting, the corrosion rate of FeCoNiCr was 7.62×10^{-4} mm/yr, whereas that of $FeCoNiCrCu_{0.5}$ was 8.89×10^{-3} mm/yr and 1.14×10^{-2} mm/yr for and FeCoNiCrCu. The poor corrosion resistance with increasing effect of Cu was observed due to its poor bonding between the other alloying elements. Thus, Cu segregates along the inter-dendrites and grain boundaries of the dendrites. Increasing Cu contents in the alloys generates Cu-rich inter-dendrite coupled with Cu-depleted dendrite phases. This accelerates the galvanic corrosion mechanism at the inter-dendrite phase due to higher cathode/anode area. The polarization test confirmed that FeCoNiCr had comparatively highest E_{corr} (−0.26 V_{SCE}) and E_{pit} (0.31 V_{SCE}) with lowest corrosion current density (3.15×10^{-8} A/cm^2). The general trend based on corrosion resistance in 3.5 % NaCl at 25 °C was 304 SS < FeCoNiCrCu < $FeCoNiCrCu_{0.5}$ < FeCoNiCr. Similar trend is observed in 1 M H_2SO_4 at 25C [210].

Eight CCAs which are CuCrFeNiMn, $CuCrFeNi_2Mn_2$, $CuCr_2Fe_2NiMn$, $CuCr_2Fe_2Ni_2Mn_2$, $Cu_2CrFe_2NiMn_2$, $Cu_2CrFe_2Ni_2Mn$, $Cu_2Cr_2FeNiMn_2$, $Cu_2Cr_2FeNi_2Mn$ were evaluated for corrosion resistance behaviour [244,245]. The alloys had dendritic and inter-dendritic structures. Although single FCC phase was expected, most of the alloys had dual phase of FCC and BCC. Generally, the alloy with the lowest Cu content and low segregation of element had the best corrosion resistance. The degree of segregation increased with increasing Cu content. High degree of segregation led to the formation of Cu-rich and Cr-depleted zones. This sets up galvanic corrosion between the inter-dendrites and dendrites, the driving force for corrosion along the inter-dendrites (intergranular corrosion) explaining the observation from the immersion test. The multi-phase structures showed greater susceptibility to corrosion. The $CuCr_2Fe_2Ni_2Mn_2$ appeared as the best (CCA) candidate in 1 M H_2SO_4.

The effect of molybdenum on the corrosion behaviour of as-cast $Co_{1.5}CrFeNi_{1.5}Ti_{0.5}Mo_x$ (x = 0, 0.1, 0.5, 0.8) in basic and acidic media at ambient temperature is studied [246,231]. The alloys were predominantly FCC crystal structure with dendrites and inter-dendritic phases as the Mo concentration varies. For Mo-free and 0.1 wt% of Mo, the dendrites and inter-dendrites were rich in Fe-Cr and Ni-Ti, whereas inter-dendrites and dendrites of 0.5 and 0.8 Mo are rich in Cr-Mo (σ) and Co-Ni phases. An overall active–passive corrosion behaviour with wide passive region (between 1109 and 1130 mV) was observed after testing as-cast $Co_{1.5}CrFeNi_{1.5}Ti_{0.5}Mo_x$ alloys in 0.5 M H_2SO_4. The presence of Mo was noted to increase i_{pass}, E_{corr} and reduce i_{corr}, i_{crit} reducing the overall corrosion resistance. This may be attributed to the reduction in the concentration of Cr in the alloys as Mo is increased. Chromium stabilizes the passive layer formed and supply continuous protection to the underlying alloy from electrochemical attack. The formation of the deleterious interdendritic Cr-Mo (σ) phase in the high Mo containing CCA may be a contributing factor for the further decrease in corrosion resistance [231]. Galvanic couple in the Cr-Mo rich σ phase coupled with Cr-Mo depleted phase led to galvanic corrosion.

The dendritic phase of $Co_{1.5}CrFeNi_{1.5}Ti_{0.5}Mo_x$ showed uniform corrosion [231]. For 1 M NaOH, the polarization results showed increasing Mo content led to reduction of the corrosion resistance. The increasing values of i_{crit} (0.20 μA/cm^2 – 0.63 μA/$cm^{2)}$ and i_{corr} with increase in Mo content showed the frequent dissolution and the porous nature of the passive layer. The $Co_{1.5}CrFeNi_{1.5}Ti_{0.5}Mo_x$ alloy also showed higher resistance to pitting corrosion in the 1 M NaCl solution. Although there was wide passive region (ΔE = 557 – 1429 mV) for the alloy in 1 M deaerated NaOH solution, increasing Mo content resulted in decreasing i_{corr} contributing to improved corrosion resistance [246]. Hence, Mo-containing alloys have excellence effect on electrochemical behaviour and susceptibility to pitting compared to Mo-free $Co_{1.5}CrFeNi_{1.5}Ti_{0.5}$ alloy [246]. As-cast $Co_{1.5}CrFeNi_{1.5}Ti_{0.5}Mo_{0.5}$ and $Co_{1.5}CrFeNi_{1.5}Ti_{0.5}Mo_{0.8}$ showed no signs of pitting corrosion in the 1 M NaCl solution. In varying concentrations of NaCl, critical pitting temperature reduced as the concentration increased [246]. The effect of the high solution temperature on the pitting behaviour was attributed to the reduction in performance of the protective oxides. Film porosity and defects in the passive film were accelerated in elevated temperatures. This caused the harmful effects of the chloride ions within the high mixed gases, chloride, and sulphide environment. Thus, localized corrosion is extremely dangerous to film as it brings about sudden catastrophic failures. Hence, alloys with high resistance to pitting is needed in most HPHT region. The Mo-containing alloy thrived in all the varying pH and chloride even at elevated temperature regions showing its superiority over the current use of 304 SS in the harsh environments of the oil and gas fields.

Early research on the effect of Ti on the widely studied AlCoCrFeNi CCA has been focused on the use of alloy as coatings. The corrosion behaviour of $Al_2CrFeNiCoCuTi_x$ coatings with the addition of Ti in molar concentrations of 0, 0.5, 1.0, 1.5, 2.0 in 0.5 mol/L HNO_3 have been studied [247]. The XRD analysis revealed the major phase of Ti-free alloy as BCC1 + FCC mixed solid solutions. As Ti increased (x = 0.5) the emergence of the BCC2 and laves phase was seen in the pre-existing phase. At x = 1, the BCC1 and BCC2 phases intensify causing laves phase to almost disappear. However, at a Ti molar concentration of 1.5, laves phase increases again whiles the BCC1 and BCC2 phases also show an increased trend. The only phase that can be seen after increasing the Ti content to 2 is BCC1 phase. This phase evolution can be used to explain the role Ti play in stabilising BCC solid solutions. The SEM and EDS characterization also revealed parallel columnar dendrite grain growth toward the direction of heat flow along with a huge increase and decrease in the Fe and Al, respectively. The higher dilution of substrate from the high energy laser beams due to high melting temperatures of constituent elements of CCA lead to the increase in Fe whiles the low melting temperature of Al aids in a higher evaporation rate. It is predicted that, a lowered Al content in the coating after bonding with substrate will increase corrosion resistance. The polarization test confirmed the prediction as an enhancement in the corrosion resistance of the CCA coating with high E_{corr} and low i_{corr} as the Ti content increased. Comparing the corrosion resistance of the substrate (Q235 steel) to the CCA coating in 0.5 M HNO_3, corrosion current is

reduced by almost 1–2 orders of magnitude; a sign of higher protection guaranteed by CCA coating. The potentiodynamic polarisation results showed that a wider passive region was seen for Ti = 1.5. Obviously, the improved corrosion resistance of the CCA with increase in Ti can be attributed to the TiO_2 stable passive layer formed. Furthermore, the role of Ti in forming a stable single phase (BCC) saw the CCA with maximum Ti content (no secondary phases) showing better corrosion resistance. Not only does the addition of Ti improve the corrosion resistance, wear and magnetization are also improved. No information on the pitting behaviour of the coating was reported but literature has shown that pitting is usually characterized by solutions with Cl^-. From the wider passive region and the absence of Cl^-, it can be expected that the alloy undergoes no pitting corrosion in the high oxidation nitric acid.

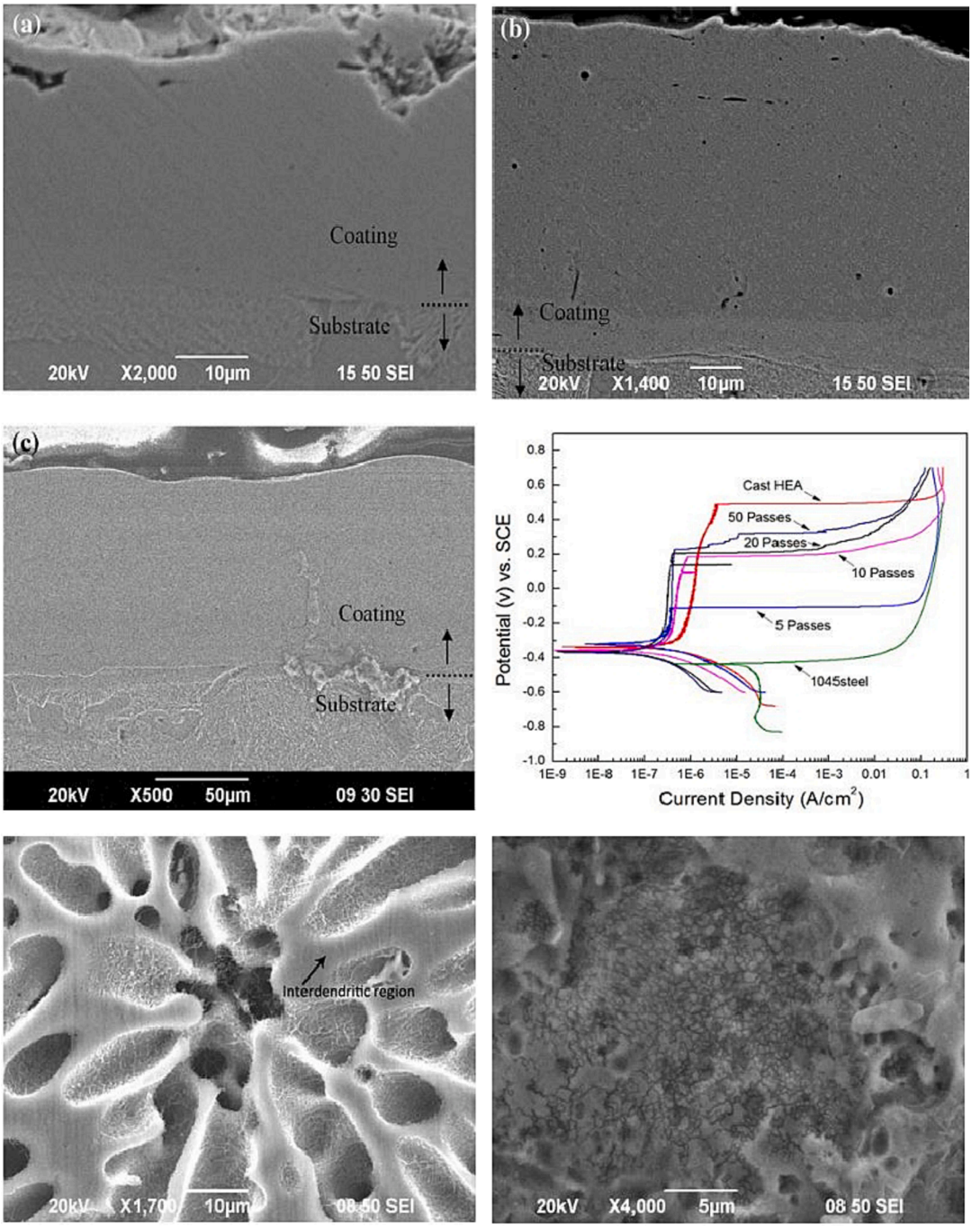

Fig. 10. SEM images showing cross-section of (a) 5-pass (b) 20-pass (c) 50-pass coatings (d) Potentiodynamic polarization curves of substrate, as-cast CCA and different pass coatings (e) and (f) comparing the corroded surfaces of the as cast CCA and the 50-pass CCA coating with uniform corrosion behaviour [242].

The effect of varying content of Ti on the electrochemical behaviour of as-cast $AlCoCrFeNiTi_x$ (x = 0, 0.4, 0.8, 1.0) have been studied [248]. Increasing Ti intensified the lattice distortion due to its large atomic radius. From this, another BCC (referred to as BCC2 due to different lattice constant) crystal structure in addition to the existing BCC (BCC1) and small laves phase was seen as molar concentration of Ti increased from 0 to 0.4. The SEM analysis confirm phases were known to consist of Ti- (Al, Ni) rich dendrite phase (DR) and nanocrystalline interdendritic structure (ID) rich in Fe and Cr (Co uniformly segregated). As Ti increased from 0.4 to 1.0, a continuous increase in the BCC2 phase was seen. Based on the composition analysis, a Cr-depleted dendrite was confirmed to form finer nanoparticles.

After subjecting all the alloys to 3.5 % NaCl, the potentiodynamic polarisation curves showed that all alloys displayed passivation with pitting being the main associated corrosion mechanism. Corrosion prefers sites with higher energies such as points of defects and grain boundaries, as a result, a reduction in these sites enhances the corrosion resistance. The initial addition of Ti to the as-cast CCA aids in the passivation process by forming TiO_2 but at higher levels, rise in grain boundaries due to increased nanoparticle formation associated with the interdendritic phase. Beside the intermetallics bound to form at higher Ti levels, potential difference between the BCC Ti-Al-Ni DR and Fe-Cr rich ID becomes obvious and sets up a driving force for corrosion. This explains the two-way behaviour of Ti on the reported CCA. $AlCoCrFeNiTi_{0.4}$ exhibited the highest corrosion potential along with the lowest free corrosion current and showed no signs of visible pitting. $AlCoCrFeNiTi_{0.8}$ and $AlCoCrFeNiTi_{1.0}$ were the most susceptible to pitting corrosion in the 3.5 % NaCl solution.

7.2. Coatings based on CCA compositions

Production of bulk CCAs has been known to be expensive. Therefore, decision to use CCA coatings on abundant and cheap, fairly corrosion resistant metal or alloy to maximize profit in oil and gas production has been adopted. The preparation techniques used in applying the CCA coatings on the substrates, their effect on the resulting microstructure has been widely studied and documented [249,250]. Various CCA coatings with superior corrosion qualities are discussed.

A recent study conducted on the behaviour of $AlCoCr_xFeNi$ (x = 0.5, 0.75, 1.0, 1.5, 2.0) coating on grade 45 steel by laser cladding in 0.1 mol/L HCl and 3.5 wt% NaCl solution [211]. The dilution rate was found to increase with an increase in x owing to the high absorptive energy and melting temperature (lower solubility limit of Cr at lower temperatures) [251]. The XRD results revealed that the CCA mostly consisted of FCC solid solution phase along with traces of $AlFe_3$, an intermetallic, confirming the dendrites and the inter-dendritic structure obtained from the microstructure analysis.

The potentiodynamic polarization test in 0.1 mol/L HCl showed that $AlCoCr_{1.5}FeNi$ provided the best corrosion resistance with a comparatively lower E_{corr} (-0.293 V), i_{pass} (3.16×10^{-6} A cm^{-2}), E_p-E_{corr} (0.090 V) together with a higher E_{bp}-E_p (0.3 V). Further analyses of the passive layer with an XPS showed that the film composed of oxides of the constituent elements [211]. Although Al_2O_3 passivates spontaneously followed by Cr_2O_3, the difficulty in dissolution of Cr_2O_3 in low pH solutions rich in Cl^- was critical in the passivity behaviour due to its dense and high resistance of about 10 Ω, indicative of the dependence of the passive film on high Cr content. The potentiodynamic test in the 3.5 wt% NaCl solution confirmed the reduction in corrosion resistance of $AlCoCr_2FeNi$ and attributed it to the sharp increase in Fe and reduction in the Al and Cr content.

A general trend of corrosion resistance was observed i.e., grade 45 steel < 304 SS [252] < $AlCoCr_{0.5}FeNi$ coating < $AlCoCr_2FeNi$ coating < $AlCoCr_{0.75}FeNi$ coating < $AlCoCr_1FeNi$ coating < $AlCoCr_{1.5}FeNi$ coating. The coatings were immersed in 0.1 $molL^{-1}$ HCl at 25C for 24 hrs. The $AlCoCr_{1.5}FeNi$ coating showed the highest resistance to pitting corrosion [211].

The electrochemical properties of AlCoCrFeNi coatings on AISI 1045 steel by electrospark process (ESP) are studied [242]. The microstructure of the coatings at different passes was compared. The coatings had simple BCC structure which was the parent structure for the substrate and the as-cast CCA. The Al-rich dendrite surrounded by Cr-rich interdendritic phase was seen for the as-cast. Aside the common observed microstructure (columnar grain growth perpendicular to the substrate surface) in all the CCA coatings, different microstructures were seen as the thickness increased with increasing the number of passes (5, 20, 50) in Fig. 10a, b, c. The 50-pass coating portrayed a narrow transition (columnar to equiaxed) zone, and an "undiluted" zone whiles the 5-pass coating exhibited highly diluted top layer [242].

Corrosion parameters were recorded after the samples tested in 3.5 wt% NaCl [242]. The potentiodynamic polarization test showed that the 5-pass ESP coating exhibited the least resistance to corrosion [242]. This is due to high dilution caused by the direct entry of Fe from substrate into the coating which may cause the formation of intermetallics. These segregated intermetallics serves as points of localized corrosion due to the absence of secondary phases. The 50-pass coatings showed the best corrosion resistance with high E_{corr} and lower i_{corr} (two orders lower than the substrate) coupled with wider passive region (~554 mV). From Fig. 10d, the 50-pass coating was the closest to providing the corrosion resistance the bulk CCA can render in a the 3.5 wt% NaCl even though all the coatings had superior corrosion resistance than the substrate. The XPS analysis confirmed that the 50-pass coating has higher peaks of oxides of Cr and Al on the surface. The SEM analysis showed uniform corrosion of the Cr-depleted dendritic phases (Fig. 10e and f) [242]. Increasing the number of passes during an ESP increases the corrosion resistance of the substrate by ensuring uniform top layer.

The $Al_xFeCoNiCuCr$ (x = 1.0–2.0) layer by laser cladding was studied [242,253]. The effect of Al on the coatings microstructure and properties have well been probed. SEM analysis revealed an Al-rich interdendritic phase along with a Cr-rich dendrite phase. However, unlike the bulk as-cast CCA, Cu segregation is not that obvious in the coatings. Loss in Al content was attributed to evaporation due to high laser power and the dissolution of the Cr-depleted interdendritic phase because of galvanic corrosion. Cu segregation was not visible as it was in the cast alloys because of the faster solidification. The phase characterization revealed intensification of BCC crystal structure with increasing Al content like the bulk CCA. The microhardness and elevated temperature hardness were found to increase with Al increase due to the high lattice distortion and the transition of FCC to BCC. BCC has higher hardness than FCC. Further results

from TEM analysis proved that the x = 1.3 had a long Widmanstätten precipitates which later progressed into spherical precipitates in the matrix as Al content in the coating increased. The elevated temperature hardness and wear resistance showed a general increase due to the formation of abundant spherical precipitates with increased Al. Surprisingly, monotonic trend was not realized as Al increased. $Al_{1.3}$FeCoNiCuCr and $Al_{1.5}$FeCoNiCuCr coatings showed the worst resistance to corrosion and best resistance to corrosion respectively in the 0.05 M HCl solution at room temperature.

8. Area for further research direction

The design of corrosion resistant alloys should meet four vital factors and critical design conditions. Among the factors are electrochemical nature of the environment, metallurgical design considerations, thermodynamics of the process to and the physical chemical interactions. Complex concentrated alloys studied so far have shown promise when tested under harsh conditions under laboratory scale. However, there are areas that require further research direction if these alloys have the potential to replace current conventional alloys.

Vast compositional spaces and rational alloy design approaches: The compositional spaces of CCAs are vast. There are continuous efforts to develop more alloy systems for functional applications, i.e., improved corrosion properties. However, existing compositions are barely optimised from composition-processing-structure–property perspectives. This is because it is an optimization challenge on multiple fronts. However, the science of designing these corrosion resistant CCAs should drive the engineering application process. Although CCAs have been developed and tested under laboratory scale with amazing structural and functional properties, the scalability and using them in actual engineering applications is still lacking. Hence it is vital for large scale testing targeting specific engineering applications are done. The importance of ensuring that current and already known systems of CCAs/HEAs are optimized using rational alloy design processes are crucial as developing new alloy systems [254]. By fine-tuning the alloy compositions, CCAs can be tailored and optimized to outperform conventional highly alloyed structural steels and Ni-based alloys.

Simulated heat treatment process and microstructural stability: The use of experimentally and computationally derived phase diagrams to understand transformation of the phases and the temperature ranges. Since high order phase diagrams for four elements and above have not been developed, the binary and ternary phase diagrams could be beneficial. This will provide the needed insight for designing a tailored corrosion and mechanical properties using carefully controlled heat treatment route. Blend of computational and empirical tools could drive the optimization of heat treatment. With commercial and proprietary machine learning based tools, density functional theory and Monte Carlo or molecular dynamics models available, most of the iterative processes associated with high throughput experimental heat treatment can be reduced [254]. Atomic-scale structural prediction under different thermal and mechanical stresses influencing the evolution of the microstructure can be resolved. Another area of importance is to understand the phase stability of CCAs under HPHT conditions. Thus, effects of temperature, pressure and exposure to various HPHT corrosive fluids can also be simulated. Insights from these critical research areas will be essential in maintaining the structural integrity and the passive layers of the CCAs at those high temperatures and pressures in the oil wells.

Testing, validation, corrosion mechanism, scalability, and cost implications: There is the need for rigorous testing, verification, and validation of CCAs in simulated HPHT environment. These conditions are critical for assessing the durability of the material under real-world scenarios. Insights from mimicking real-world scenarios can be used to design protocols for effective evaluation of long-term durability, corrosion, and mechanical properties. The laboratory scale tests can be complimentary to the field tests and trials for actual performance validation in typical oil and gas environments. The approach can be used to gain insights and elucidate the corrosion mechanisms of the alloys. Direct assessment of the passive film formed, the distribution of elements and the interaction of various organic and inorganic substance can be studied. This could provide deep understanding of the material-method-mechanisms guidelines for robust design of corrosion resistance CCAs for HPHT environments.

The current development of CCAs is still at the laboratory scale. There is the need for transition to industrial application which requires scalability [166,168,169]. This opens for research in understanding some of the conditions, processes, and cost-effective models for scale-up. A critical area for cost benefit analysis is the techno-economic assessment and the market research analyses of viable CCA industry. This could generate an understanding around the economic feasibility of using CCAs for HPHT wells and factors that could facilitate or hinder their adoption and use in the oil and gas industry. The goal is to aid the explicability of any claims to minimize negative impacts of CCAs and provide guidance for societal impact-informed alloy design.

9. Conclusion

Structural and functional applications of the next generation of materials require improved mechanical, physical and corrosion properties. This is to reduce the overall failure rate of structural and functional components through mechanical fatigue, wear, corrosion, and corrosion fatigue. Within the high-pressure high temperature environments, ~60 % of all failure cases reported between 2009 and 2018 are corrosion and material related. Thus, conditions necessitating the aggressive and harsh corrosion environments with the two main types of corrosion are discussed. Current conventional corrosion resistant alloys and mitigating perspectives are also highlighted and discussed. Limitations of these conventional alloys from ambient and elevated temperatures from corrosion perspectives are reviewed. Emphasis has been on conventional corrosion resistance alloys, which are stainless steels and low alloyed carbon steels used for HPHT applications. Due to the relative high pressures and temperatures, corrosion enhanced organic inhibitors are not applicable. The potential applications of complex concentrated alloys (CCAs) for mitigating sweet and sour corrosion in HPHT oil and gas wells are reviewed. The harsh and aggressive conditions in HPHT wells such as concentrated chlorides, carbon dioxide, and hydrogen sulphides and their effects on structural integrity were also discussed.

Most CCAs have high resistance to general and pitting corrosion compared to conventional alloys such as stainless steel. The better corrosion resistance of CCAs than stainless steels is attributed to the cocktail effects of the constituent elements. Reduction in corrosion resistance of CCAs in both chloride and H_2SO_4 environments are due to increasing Fe contents at the expense of Al and Cr contents. The effect of Al and Cr on the corrosion resistance of CCAs had same characteristics to stainless steels. However, there is still the need to further optimize their elemental compositions to produce corrosion resistant CCAs with better cocktail of structural and functional properties than current corrosion resistant alloys in mitigating sweet and sour corrosion in HPHT environments. The thermodynamic information is unsatisfactory and hence future works should target the kinetics of the oxides formation and how they interact in the presence of the other oxides in aqueous, acidic, and basic solutions of different concentrations.

Areas for future research directions are highlighted. These include optimization of current corrosion resistant CCA compositions, phase stability of microstructures, understanding the mechanisms, designing and standardization of lab-scale and field test protocols and scaling up with emphasis on cost implication. Finally, the insight from current CCAs and the suggested areas for future research direction are essential for the future of structural and functional component designs.

CRediT authorship contribution statement

D.E.P. Klenam: Conceptualization, Methodology, Formal analysis, Investigation, Writing – original draft, Writing - review & editing. **F. McBagonluri:** Resources, Writing – review & editing. **O.S. Bamisaye:** Writing – original draft, Methodology, Investigation, Writing – review & editing. **T.K. Asumadu:** Conceptualization, Methodology, Formal Analysis, Investigation, Writing – review & editing. **N.K. Ankah:** Writing – original draft, Investigation, Formal Analysis, Writing – review & editing. **M.O. Bodunrin:** Conceptualization, Methodology, Investigation, Writing – original draft, Writing - review & editing. **A. Andrews:** Project administration, Resources, Supervision, Writing – review & editing. **W.O. Soboyejo:** Conceptualization, Supervision, Writing – review & editing, Project administration, Resources.

Declaration of competing interest

The authors declare that they have no known competing financial interests or personal relationships that could have appeared to influence the work reported in this paper.

Data availability

Data will be made available on request.

References

[1] X.Q. Pang, C.Z. Jia, W.Y. Wang, Petroleum geology features and research developments of hydrocarbon accumulation in deep petroliferous basins, Pet. Sci. 12 (1) (2015) 1–53, https://doi.org/10.1007/s12182-015-0014-0.
[2] M. Iannuzzi, A. Barnoush, R. Johnsen, Materials and corrosion trends in offshore and subsea oil and gas production, Npj Mater. Degrad. 1 (1) (2017) 1–11.
[3] N. Sridhar, R. Thodla, F. Gui, L. Cao, A. Anderko, Corrosion-resistant alloy testing and selection for oil and gas production, Corros. Eng. Sci. Technol. 53 (2018) 75–89.
[4] M. Kappes, M. Iannuzzi, R.B. Rebak, R.M. Carranza, Sulfide stress cracking of nickel-containing low-alloy steels, Corros. Rev. 32 (3–4) (2014) 101–128.
[5] L.D. Paolinelli, B. Brown, S.N. Simison, S. Nesic, Inhibition of CO 2 corrosion of carbon steel with 1% Cr, Mater Chem Phys 136 (2–3) (Oct. 2012) 1092–1102, https://doi.org/10.1016/j.matchemphys.2012.08.055.
[6] Y.S. Choi, D. Young, S. Nešić, L.G.S. Gray, Wellbore integrity and corrosion of carbon steel in CO2 geologic storage environments: A literature review, Int. J. Greenhouse Gas Control 16 (2013), https://doi.org/10.1016/j.ijggc.2012.12.028.
[7] F. Farelas, M. Galicia, B. Brown, S. Nesic, H. Castaneda, Evolution of dissolution processes at the interface of carbon steel corroding in a CO2 environment studied by EIS, Corros Sci 52 (2) (Feb. 2010) 509–517, https://doi.org/10.1016/j.corsci.2009.10.007.
[8] O. Palumbo, A. Paolone, P. Rispoli, R. Cantelli, G. Cannelli, S. Nesic, B.J. Molinas, P.P. Zonta, Anelastic spectroscopy study of iron carbonate scales from CO2 corrosion of steel, Mater. Sci. Eng. A 521–522 (Sep. 2009) 343–346, https://doi.org/10.1016/j.msea.2008.09.091.
[9] S. Nešić, Key issues related to modelling of internal corrosion of oil and gas pipelines - A review, Corros Sci 49 (12) (Dec. 2007) 4308–4338, https://doi.org/10.1016/j.corsci.2007.06.006.
[10] Y. Zheng, B. Brown, S. Nesic, "Electrochemical study and modeling of H2S corrosion of mild steel", in NACE International, Corrosion (2013) 1–22.
[11] Y.S. Choi, S. Nesic, S. Ling, Effect of H2S on the CO2 corrosion of carbon steel in acidic solutions, Electrochim Acta 56 (4) (Jan. 2011) 1752–1760, https://doi.org/10.1016/j.electacta.2010.08.049.
[12] M. Nordsveen, S. Nesic, R. Nyborg, A. Stangeland, A Mechanistic Model for Carbon Dioxide Corrosion of Mild Steel in the Presence of Protective Iron Carbonate Films-Part 1: Theory and Verification, Corrosion 59 (5) (2003) 443–456.
[13] M. Koyama, M. Rohwerder, C.C. Tasan, A. Bashir, E. Akiyama, K. Takai, D. Raabe, K. Tsuzaki, A recent progress in microstructural hydrogen mapping in steels: Quantification, kinetic analysis, and multi-scale characterization, Mater. Sci. Technol. 13 (13) (2017) 1481–1496, https://doi.org/10.1080/02670836.2017.129927.
[14] D.E.P. Klenam, M.O. Bodunrin, S. Akromah, E. Gikunoo, A. Andrews, F. McBagonluri, Ferrous materials degradation: Characterisation of rust by colour-an overview, Corros. Rev. 39 (4) (2021) 297–311.
[15] M.O. Bodunrin, L.H. Chown, J.W. van der Merwe, K.K. Alaneme, C. Oganbule, D.E.P. Klenam, N.P. Mphasha, Corrosion behavior of titanium alloys in acidic and saline media: Role of alloy design, passivation integrity, and electrolyte modification, Corros. Rev. 38 (1) (2020) 25–47.
[16] I. B. Obot, I. B. Onyeachu, S. A. Umoren, M. A. Quraishi, A. A. Sorour, T. Chen, N. Aljeaban, and Q. Wang, "High temperature sweet corrosion and inhibition in the oil and gas industry: Progress, challenges and future perspectives," *J Pet Sci Eng*, vol. 185, no. August 2019, p. 106469, 2020.
[17] K. Haruna, I.B. Obot, N.K. Ankah, A.A. Sorour, T.A. Saleh, Gelatin : A green corrosion inhibitor for carbon steel in oil well acidizing environment, J Mol Liq 264 (2018) 515–525.
[18] A. Groysman, "Corrosion problems and solutions in oil , gas , refining and petrochemical industry Korozní problémy při zpracování plynu a ropy," pp. 100–117, 2017.

[19] P.R. Rhodes, L.A. Skogsberg, R.N. Tuttle, Pushing the limits of metals in corrosive oil and gas well environments, Corrosion 63 (1) (2007) 63–100, https://doi.org/10.5006/1.3278334.
[20] C.I. Ossai, "Advances in Asset Management Techniques : An Overview of Corrosion Mechanisms and Mitigation Strategies for Oil and Gas Pipelines", International Scholarly Research, Network (2012) 1–10, https://doi.org/10.5402/2012/570143.
[21] A.M. Nejad, A review of contributing parameters in corrosion of oil and gas wells, Anti-Corros. Methods Mater. 65 (1) (2018) 73–78, https://doi.org/10.1108/ACMM-03-2017-1779.
[22] J.J. Demo, A.P. Bons, Intergranular Corrosion and Embrittlement of Ferritic Stainless Steels, Corrosion 31 (1) (1975) 21–22.
[23] E.P. George, D. Raabe, R.O. Ritchie, High-entropy alloys, Nat Rev Mater 4 (8) (2019) 515–534.
[24] B. Cantor, I.T.H. Chang, P. Knight, A.J.B. Vincent, Microstructural development in equiatomic multicomponent alloys, Mater. Sci. Eng. A 375–377 (Jul. 2004) 213–218.
[25] J.W. Yeh, S.K. Chen, S.J. Lin, J.Y. Gan, T.S. Chin, T.T. Shun, C.H. Tsau, S.Y. Chang, Nanostructured high-entropy alloys with multiple principal elements: Novel alloy design concepts and outcomes, Adv Eng Mater 6 (5) (2004) 299–303.
[26] S. Zhang, Y. Li, B. Liu, L. Mou, S. Yu, Y. Zhang, X. Yan, Understanding the synergistic effect of CO2, H2S and fluid flow towards carbon steel corrosion, Vacuum 196 (Feb. 2022), https://doi.org/10.1016/j.vacuum.2021.110790.
[27] I. B. Obot, A. A. Sorour, C. Verma, T. A. Al-Khaldi, and A. S. Rushaid, "Key parameters affecting sweet and sour corrosion: Impact on corrosion risk assessment and inhibition," *Engineering Failure Analysis*, vol. 145. Elsevier Ltd, Mar. 01, 2023. doi: 10.1016/j.engfailanal.2022.107008.
[28] M. Wasim and M. B. Djukic, "External corrosion of oil and gas pipelines: A review of failure mechanisms and predictive preventions," *Journal of Natural Gas Science and Engineering*, vol. 100. Elsevier B.V., Apr. 01, 2022. doi: 10.1016/j.jngse.2022.104467.
[29] Z. Wang, H. Lu, J. Cai, L. Wu, K. Luo, J. Lu, Improvement mechanism in stress corrosion resistance of the X70 pipeline steel in hydrogen sulfide solution by massive laser shock peening treatment, Corros Sci 201 (Jun. 2022), https://doi.org/10.1016/j.corsci.2022.110293.
[30] L. Chen, R. Case, L. Liu, S. Xiang, H. Castaneda, Assessment of sulfide corrosion cracking and hydrogen permeation behavior of ultrafine grain high strength steel, Corros Sci 198 (Apr. 2022), https://doi.org/10.1016/j.corsci.2022.110142.
[31] Y. Long, W. Song, A. Fu, J. Xie, Y. Feng, Z. Bai, C. Yin, Q. Ma, N. Ji, X. Kuang, Combined effect of hydrogen embrittlement and corrosion on the cracking behaviour of C110 low alloy steel in O2-contaminated H2S environment, Corros Sci 194 (Jan. 2022), https://doi.org/10.1016/j.corsci.2021.109926.
[32] Y. Qiu, M.A. Gibson, H.L. Fraser, N. Birbilis, Corrosion characteristics of high entropy alloys, Mater. Sci. Technol. 31 (10) (2015) 1235–1243.
[33] Y. Qiu, S. Thomas, M.A. Gibson, H.L. Fraser, N. Birbilis, Corrosion of high entropy alloys, Npj Mater Degrad 1 (1) (2017) 1–17.
[34] X.W. Qiu, Y.P. Zhang, L. He, C.G. Liu, Microstructure and corrosion resistance of AlCrFeCuCo high entropy alloy, J Alloys Compd 549 (2013) 195–199, https://doi.org/10.1016/j.jallcom.2012.09.091.
[35] Y.J. Hsu, W.C. Chiang, J.K. Wu, Corrosion behavior of FeCoNiCrCux high-entropy alloys in 3.5% sodium chloride solution, Mater Chem Phys 92 (1) (2005) 112–117, https://doi.org/10.1016/j.matchemphys.2005.01.001.
[36] S. Shuang, Z.Y. Ding, D. Chung, S.Q. Shi, Y. Yang, Corrosion resistant nanostructured eutectic high entropy alloy, Corros Sci 164 (Mar. 2020).
[37] Y. Shi, B. Yang, and P. K. Liaw, "Corrosion-resistant high-entropy alloys: A review," *Metals*, vol. 7, no. 2. MDPI AG, Feb. 01, 2017. doi: 10.3390/met7020043.
[38] S.S. Nene, M. Frank, K. Liu, S. Sinha, R.S. Mishra, B.A. McWilliams, K.C. Cho, Corrosion-resistant high entropy alloy with high strength and ductility, Scr Mater 166 (2019) 168–172.
[39] A. S. M. Ang and C. C. Berndt, "A review of testing methods for thermal spray coatings," *International Materials Reviews*, vol. 59, no. 4. Maney Publishing, pp. 179–223, 2014. doi: 10.1179/1743280414Y.0000000029.
[40] A. Sova, M. Doubenskaia, E. Trofimov, and M. Samodurova, "Deposition of High-Entropy Alloy Coating by Cold Spray Combined with Laser Melting: Feasibility Tests," *Journal of Thermal Spray Technology*, vol. 31, no. 4. Springer, pp. 1112–1128, Apr. 01, 2022. doi: 10.1007/s11666-021-01300-0.
[41] A. Moridi, S. M. Hassani-Gangaraj, M. Guagliano, and M. Dao, "Cold spray coating: Review of material systems and future perspectives," *Surface Engineering*, vol. 30, no. 6. Maney Publishing, pp. 369–395, 2014. doi: 10.1179/1743294414Y.0000000270.
[42] Q. Wang, P. Han, S. Yin, W. J. Niu, L. Zhai, X. Li, X. Mao, and Y. Han, "Current research status on cold sprayed amorphous alloy coatings: A review," *Coatings*, vol. 11, no. 2. MDPI AG, pp. 1–21, Feb. 01, 2021. doi: 10.3390/coatings11020206.
[43] R. Ghelichi, S. Bagherifard, M. Guagliano, M. Verani, Numerical simulation of cold spray coating, Surf Coat Technol 205 (23–24) (Sep. 2011) 5294–5301, https://doi.org/10.1016/j.surfcoat.2011.05.038.
[44] A. Fardan, C.C. Berndt, R. Ahmed, Numerical modelling of particle impact and residual stresses in cold sprayed coatings: A review, Surf Coat Technol (2021) 126835.
[45] N. Birbilis, S. Choudhary, J. R. Scully, and M. L. Taheri, "A perspective on corrosion of multi-principal element alloys," *npj Materials Degradation*, vol. 5, no. 1. Nature, Dec. 01, 2021. doi: 10.1038/s41529-021-00163-8.
[46] C.B. Nascimento, U. Donatus, C.T. Ríos, M.C.L. De Oliveira, R.A. Antunes, A review on Corrosion of High Entropy Alloys: Exploring the Interplay between Corrosion Properties, Alloy Composition, Passive Film Stability and Materials Selection, Mater. Res. 25 (2022), https://doi.org/10.1590/1980-5373-MR-2021-0442.
[47] G. Zhang, H. Liu, X. Tian, P. Chen, H. Yang, J. Hao, Microstructure and Properties of AlCoCrFeNiSi High-Entropy Alloy Coating on AISI 304 Stainless Steel by Laser Cladding, J Mater Eng Perform (2019) 1–11, https://doi.org/10.1007/s11665-020-04586-3.
[48] A.P. Kidnay, *Fundamentals of Natural Gas Processing*, 2nd Editio, CRC Press Taylor & Francis Group, Boca Raton, 1995.
[49] T. Smithson, HPHT Wells, Oilfield Review (2016) 1–2.
[50] D.J. Lehr, S.D. Collins, The high-pressure/high-temperature completion landscape - yesterday, today and tomorrow, SPE Drill. Complet (2015) 187–197.
[51] M. Payne, Technology Focus: HP/HT challenges, J. Petrol. Tech. 62 (04) (2010) 70.
[52] P.D. Pathak, C.G. Kocurek, S.L. Taylor, Design Method Combining API and ASME Codes for Subsea Equipment for HP/HT Conditions Up to 25,000-psi Pressure and 400°F Temperature, Oil and Gas Facilities 3 (02) (2014) 47–55.
[53] M. B. Kermani and D. Harrop, "Impact of corrosion on oil and gas industry," *Proceedings of the Middle East Oil Show*, vol. 1. pp. 135–148, 1995.
[54] A. Alviz-Meza, S.I. Shah, V. Kafarov, D.Y. Peña-Ballesteros, Fireside corrosion of 9Cr-1Mo steel at high temperatures, in the acid flue gas from an oil refinery, Corros Sci 193 (Dec. 2021), https://doi.org/10.1016/j.corsci.2021.109878.
[55] A. H. Alamri, "Localized corrosion and mitigation approach of steel materials used in oil and gas pipelines – An overview," *Engineering Failure Analysis*, vol. 116. Elsevier Ltd, Oct. 01, 2020. doi: 10.1016/j.engfailanal.2020.104735.
[56] M.F. Shehata, A.M. El-Shamy, Hydrogen-based failure in oil and gas pipelines a review, Gas Science and Engineering 115 (Jul. 2023) 204994, https://doi.org/10.1016/j.jgsce.2023.204994.
[57] J. Fang, X. Cheng, H. Gai, S. Lin, H. Lou, Development of machine learning algorithms for predicting internal corrosion of crude oil and natural gas pipelines, Comput Chem Eng 177 (Sep. 2023), https://doi.org/10.1016/j.compchemeng.2023.108358.
[58] M. H. Sliem, E. M. Fayyad, A. M. Abdullah, N. A. Younan, N. Al-Qahtani, F. F. Nabhan, A. Ramesh, N. Laycock, M. P. Ryan, M. Maqbool, and D. Arora, "Monitoring of under deposit corrosion for the oil and gas industry: A review," *Journal of Petroleum Science and Engineering*, vol. 204. Elsevier B.V., Sep. 01, 2021. doi: 10.1016/j.petrol.2021.108752.
[59] F. Nasirpouri, A. Mostafaei, L. Fathyunes, R. Jafari, Assessment of localized corrosion in carbon steel tube-grade AISI 1045 used in output oil-gas separator vessel of desalination unit in oil refinery industry, Eng Fail Anal 40 (2014) 75–88, https://doi.org/10.1016/j.engfailanal.2014.02.012.
[60] R. Pourazizi, M. A. Mohtadi-Bonab, and J. A. Szpunar, "Investigation of different failure modes in oil and natural gas pipeline steels," *Engineering Failure Analysis*, vol. 109. Elsevier Ltd, Jan. 01, 2020. doi: 10.1016/j.engfailanal.2020.104400.
[61] G. Mubarak, C. Verma, I. Barsoum, A. Alfantazi, and K. Y. Rhee, "Internal corrosion in oil and gas wells during casings and tubing: Challenges and opportunities of corrosion inhibitors," *Journal of the Taiwan Institute of Chemical Engineers*, vol. 150. Taiwan Institute of Chemical Engineers, Sep. 01, 2023. doi: 10.1016/j.jtice.2023.105027.

[62] M.V. Biezma, M.A. Andrés, D. Agudo, E. Briz, Most fatal oil & gas pipeline accidents through history: A lessons learned approach, Eng Fail Anal 110 (Mar. 2020), https://doi.org/10.1016/j.engfailanal.2020.104446.
[63] I.B. Obot, I.B. Onyeachu, S.A. Umoren, M.A. Quraishi, A.A. Sorour, T. Chen, N. Aljeaban, Q. Wang, High temperature sweet corrosion and inhibition in the oil and gas industry: Progress, challenges and future perspectives, J Pet Sci Eng 185 (Feb. 2020), https://doi.org/10.1016/j.petrol.2019.106469.
[64] V. S. Saji and S. A. Umoren, *Corrosion inhibitors in the oil and gas industry*, 1st Editio. Weinheim: Wiley-VCHVerlag GmbH& Co. KGaA, 2020. doi: 10.1002/9783527822140.
[65] L.T. Popoola, A.S. Grema, G.K. Latinwo, B. Gutti, "Corrosion problems during oil and gas production and its mitigation", International Journal of Industrial, Chemistry (2013) 1–15.
[66] K. Nalli, Corrosion and Its mitigation in the oil and gas industries, Process Plant Equipment (2012) 673–679.
[67] M.B. Kermani, D. Harrop, The impact of corrosion on the oil and gas industry, SPE Prod. Facil. 11 (3) (1996) 186–190.
[68] M. Al Kindi, "Oilfield Corrosion : Sweet Corrosion Scales," 2020.
[69] G. H. Koch, M. P. H. Brongers, N. G. Thompson, Y. P. Virmani, and J. H. Payer, "'Corrosion Costs and Preventive Strategies in the United States,'" 2002.
[70] F.O. Kolawole, S.K. Kolawole, J.O. Agunsoye, Mitigation of Corrosion Problems in API 5L Steel Pipeline – A Review, Journal of Materials and Environmental Science 9 (8) (2018) 2397–2410.
[71] P. Roffey, E.H. Davies, The generation of corrosion under insulation and stress corrosion cracking due to sulphide stress cracking in an austenitic stainless steel hydrocarbon gas pipeline, Eng Fail Anal 44 (2014) 148–157, https://doi.org/10.1016/j.engfailanal.2014.05.004.
[72] K. Li, Y. Zeng, J.L. Luo, Influence of H2S on the general corrosion and sulfide stress cracking of pipelines steels for supercritical CO2 transportation, Corros Sci 190 (Sep. 2021), https://doi.org/10.1016/j.corsci.2021.109639.
[73] G. Jia, M. Lei, M. Li, W. Xu, R. Li, Y. Lu, M. Cai, "Hydrogen embrittlement in hydrogen-blended natural gas transportation systems: A review", International Journal of Hydrogen Energy, Elsevier Ltd (2023), https://doi.org/10.1016/j.ijhydene.2023.04.266.
[74] I.B. Obot, M.M. Solomon, S.A. Umoren, R. Suleiman, M. Elanany, N.M. Alanazi, A.A. Sorour, Progress in the development of sour corrosion inhibitors: Past, present, and future perspectives, J. Ind. Eng. Chem. 79 (2019) 1–18, https://doi.org/10.1016/j.jiec.2019.06.046.
[75] H. Asahi, Y. Sogo, M. Ueno, H. Higashiyama, Metallurgical factors controlling SSC resistance of high-strength, low-alloy steels, Corrosion 45 (6) (1989) 519–527.
[76] M. Ueda, "2006 F . N . Speller Award Lecture : Development of Corrosion-Resistance Alloys for the Oil and Gas Industry — Based on Spontaneous Passivity Mechanism," no. October, pp. 856–867, 2006.
[77] P. Rajeev, A.O. Surendranathan, C.S.N. Murthy, Corrosion mitigation of the oil well steels using organic inhibitors-A review, Journal of Materials and Environmental Science 3 (5) (2012) 856–869.
[78] A. Iversen, "Sheir's Corrosion," pp. 1802–1877, 2010.
[79] J.R. Galvele, Surface mobility mechanism of stress-corrosion cracking, Corros Sci 35 (1–4) (1993) 419–434.
[80] J. Beavers, T.A. Bubenik, Stress corrosion cracking, Trends in Oil and Gas Corrosion Research and Technologies: Production and Transmission 48 (2017) 295–314.
[81] D.A. Jones, A unified mechanism of stress corrosion and corrosion fatigue cracking, Metall. Trans. A 2 (1985) 1133–1141.
[82] E. E. Heaver, "Stress corrosion cracking of steels in industrial process environments," 1994.
[83] A. King, G. Johnson, D. Engelberg, W. Ludwig, and J. Marrow, "Observations of intergranular stress corrosion cracking in a grain-mapped polycrystal," *Science (1979)*, vol. 321, no. 5887, pp. 382–385, Jul. 2008, doi: 10.1126/science.1156211.
[84] M. Kowaka, S. Nagata, Stress corrosion cracking of mild and low alloy steels in CO-CO2-H2O environments, Corrosion 32 (10) (1976) 395–401.
[85] D.D. Macdonald, M. Urquidi-Macdonald, A couple environment model for stress corrosion cracking in sensitized type 304 stainles steel in LWR environments, Corros Sci vol. 32, no. l (1991) 51–81.
[86] M.R. Louthan, R.E. Swanson, Material defects, gas purity and hydrogen embrittlement, Int J Hydrogen Energy 10 (7–8) (1985) 551–554.
[87] H. Luo, Z. Li, W. Lu, D. Ponge, D. Raabe, Hydrogen embrittlement of an interstitial equimolar high-entropy alloy, Corros Sci 136 (May 2018) 403–408, https://doi.org/10.1016/j.corsci.2018.03.040.
[88] M. Monnot, R.P. Nogueira, V. Roche, G. Berthomé, E. Chauveau, R. Estevez, M. Mantel, Sulfide stress corrosion study of a super martensitic stainless steel in H 2 S sour environments: Metallic sulfides formation and hydrogen embrittlement, Appl Surf Sci 394 (Feb. 2017) 132–141, https://doi.org/10.1016/j.apsusc.2016.10.072.
[89] P. Bai, J. Zhou, B. Luo, S. Zheng, C. Chen, Roles of carbon dioxide and steam on the hydrogen embrittlement of 3Cr tube steel in synthetic natural gas environment, Corros. Eng. Sci. Technol. 53 (1) (2018) 1–10.
[90] H. Luo, W. Lu, X. Fang, D. Ponge, Z. Li, D. Raabe, Beating hydrogen with its own weapon: Nano-twin gradients enhance embrittlement resistance of a high-entropy alloy, Mater. Today 21 (10) (Dec. 2018) 1003–1009, https://doi.org/10.1016/j.mattod.2018.07.015.
[91] S. C. Silva, A. B. Silva, and J. A. C. Ponciano Gomes, "Hydrogen embrittlement of API 5L X65 pipeline steel in CO2 containing low H2S concentration environment," *Eng Fail Anal*, vol. 120, no. November 2020, p. 105081, 2021.
[92] H. Ma, L. Sun, H. Luo, and X. Li, "Hydrogen embrittlement of high-strength marine steel as a weld joint in artificial seawater under cathodic polarization," *Eng Fail Anal*, vol. 134, no. November 2021, p. 106044, 2022.
[93] T.E. Perez, "Corrosion in the Oil and Gas Industry : An Increasing Challenge for, Materials" 65 (8) (2013) 1033–1042, https://doi.org/10.1007/s11837-013-0675-3.
[94] J.O.M. Bockris, D. Drazic, A.R. Despic, The electrode kinetics of the deposition and dissolution of iron, Electrochim Acta 4 (2–4) (1961) 325–361, https://doi.org/10.1016/0013-4686(61)80026-1.
[95] A. Khan, A. Qurashi, W. Badeghaish, M.N. Noui-mehidi, M.A. Aziz, Frontiers and Challenges in Electrochemical Corrosion Monitoring; Surface and Downhole Applications, Sensors 20 (6583) (2020) 1–35.
[96] B.R. Linter, G.T. Burstein, Reactions of pipeline steels in carbon dioxide solutions, Corros Sci 41 (1) (1999) 117–139, https://doi.org/10.1016/S0010-938X(98)00104-8.
[97] A. Wieckowski, E. Ghali, M. Szlarczyk, J. Sobkowski, The Behaviour of Iron Electrode in Co2- Saturated Neutral Electrolyte-I. Electrochemical Study, Electrochim Acta 28 (11) (1983) 1619–1626.
[98] C. De Waard, D.E. Milliams, Carbonic Acid Corrosion of Steel, Corrosion-Nace 31 (5) (1975) 177–181.
[99] M. Al Kindi, Oilfield Corrosion : Sweet Corrosion Scales, University of Manchester, 2020.
[100] Y. Hua, S. Xu, Y. Wang, W. Taleb, J. Sun, L. Zhang, R. Barker, A. Neville, The formation of FeCO3 and Fe3O4 on carbon steel and their protective capabilities against CO2 corrosion at elevated temperature and pressure, Corros Sci 157 (Aug. 2019) 392–405, https://doi.org/10.1016/j.corsci.2019.06.016.
[101] C. Wang, Y. Hua, S. Nadimi, Q. Hu, W. Taleb, J. Zhang, X. Liu, R. Zhang, X. Chen, A. Neville, Y. Li, Anti-corrosion characteristics of FeCO3 and FexCayMgzCO3 scales on carbon steel in high-PT CO2 environments, Chem. Eng. J. 431 (Mar. 2022), https://doi.org/10.1016/j.cej.2021.133484.
[102] M. Xu, W. Li, Y. Zhou, X.X. Yang, Z. Wang, Z. Li, Effect of pressure on corrosion behavior of X60, X65, X70, and X80 carbon steels in water-unsaturated supercritical CO2 environments, Int. J. Greenhouse Gas Control 51 (Aug. 2016) 357–368, https://doi.org/10.1016/j.ijggc.2016.06.002.
[103] H. Mansoori, D. Young, B. Brown, and M. Singer, "Influence of calcium and magnesium ions on CO2 corrosion of carbon steel in oil and gas production systems - A review," *Journal of Natural Gas Science and Engineering*, vol. 59. Elsevier B.V., pp. 287–296, Nov. 01, 2018. doi: 10.1016/j.jngse.2018.08.025.
[104] B.J. Usman, S.A. Ali, Carbon Dioxide Corrosion Inhibitors: A review, Arab J Sci Eng 43 (1) (2018) 1–22, https://doi.org/10.1007/s13369-017-2949-5.
[105] P. Barnes, "An Investigation into the Corrosion Fatigue Behaviour of High Strength Carbon Steel Tensile Armour Wires Table of Contents," p. 221, 2014.
[106] A. Dugstad, "Mechanism of protective film formation during CO2 corrosion of carbon steel," *Institute of Energy Technology*, no. 31, 2007.
[107] R.C. Newman, The dissolution and passivation kinetics of stainless alloy containing molybdenum - II: dissolution kinetics in artificial pits, Corros Sci 25 (5) (1985) 341–350.
[108] N.J. Laycock, J. Stewart, R.C. Newman, The initiation of crevice corrosion in stainless steels, Corros Sci 39 (10–11) (1997) 1791–1809.

[109] A.J. Betts, R.C. Newman, The effect of alloyed molybdenum on the activation of anodic dissolution by reduced sulphur compounds, Corros Sci 34 (9) (1993) 1551–1555.
[110] V.M. Salinas-Bravo, R.C. Newman, An alternative method to determine critical pitting temperature of stainless steels in ferric chloride solution, Corros Sci 36 (1) (1994) 67–77.
[111] N.J. Laycock, R.C. Newman, J. Stewart, The transpassive corrosion of stainless steel in stabilized alkaline peroxide solution, Corros Sci 37 (10) (1995) 1637–1642.
[112] B. Lynch, Z. Wang, L. Ma, E.-M. Paschalidou, F. Wiame, V. Maurice, P. Marcus, Passivation-Induced Cr and Mo Enrichments of 316L Stainless Steel Surfaces and Effects of Controlled Pre-Oxidation, J Electrochem Soc 167 (14) (Nov. 2020) 141509, https://doi.org/10.1149/1945-7111/abc727.
[113] I. Samusawa, D. Izumi, J. Shimamura, Influence of dislocation on sour corrosion of carbon steel in a low H2S sour environment, Mater. Corros. 73 (2) (Feb. 2022) 272–280, https://doi.org/10.1002/maco.202112745.
[114] S. Gao, P. Jin, B. Brown, D. Young, S. Nesic, M. Singer, M. Technology, Corrosion behavior of mild steel in sour environments at elevated temperatures, NACE Corrosion Conference 9084 (2017) 1–17.
[115] I. B. Obot, M. M. Solomon, S. A. Umoren, R. Suleiman, M. Elanany, N. M. Alanazi, and A. A. Sorour, *Progress in the development of sour corrosion inhibitors: Past, present, and future perspectives*, vol. 79. 2019, pp. 1–18. doi: 10.1016/j.jiec.2019.06.046.
[116] C. Mendibide, T. Sourmail, Composition optimization of high-strength steels for sulfide stress cracking resistance improvement, Corros Sci 51 (12) (Dec. 2009) 2878–2884, https://doi.org/10.1016/j.corsci.2009.08.013.
[117] C.M. Hansson, The impact of corrosion on society, Metall Mater Trans A Phys Metall Mater Sci 42 (10) (2011) 2952–2962, https://doi.org/10.1007/s11661-011-0703-2.
[118] V.S. Saji, A Review on Recent Patents in Corrosion Inhibitors, Recent Patents on Corrosion Science 2 (1) (2010) 6–12, https://doi.org/10.2174/1877610810010020006.
[119] S. Papavinasam, The Main Environmental Factors Influencing Corrosion, Gulf Professional Publishing (2014), https://doi.org/10.1016/b978-0-12-397022-0.00004-2.
[120] S. Papavinasam, Mitigation – External Corrosion, London: Elseiver (2014), https://doi.org/10.1016/b978-0-12-397022-0.00009-1.
[121] B.D. Craig, L. Smith, Corrosion Resistant Alloys (CRAs) in the oil and gas industry – selection guidelines update, Nickel Institute Technical Series 0073 (2011) 1–10.
[122] S. K. Kolawole, F. O. Kolawole, A. B. O. Soboyejo, and W. O. Soboyejo, "Modeling studies of corrosion fatigue in a low carbon steel," *Cogent Eng*, vol. 6, no. 1, 2019.
[123] S.K. Kolawole, F.O. Kolawole, O.P. Enegela, O.O. Adewoye, A.B.O. Soboyejo, W.O. Soboyejo, Pitting Corrosion of a Low Carbon Steel in Corrosive Environments: Experiments and Models, Adv Mat Res 1132 (2015) 349–365.
[124] V. S. Saji, "Progress in rust converters," *Prog Org Coat*, vol. 127, no. October 2018, pp. 88–99, 2019, doi: 10.1016/j.porgcoat.2018.11.013.
[125] A. Jenkins, M. Swaco, The Challenges Associated with the Development and Application of Oil and Gas Corrosion Inhibitors, in: In *SPE International Oilfield Corrosion Conference and Exhibition*, 2014, pp. 1–13.
[126] C.H.M. Jenkins, E.H. Bucknall, C.R. Austin, G.A. Mellor, Some alloys for use at high temperatures. Part IV: The Constitution of the Alloys of Nickel, Chromium and Iron, Journal of Iron and Steel Institute 136 (1937) 187–222.
[127] A.H. Al-Moubaraki, I.B. Obot, Top of the line corrosion: causes, mechanisms, and mitigation using corrosion inhibitors, Arab. J. Chem. 14 (5) (2021) 103116.
[128] S. Cao, F. He, J. Gao, Corrosion problems in the oil country tubular goods and their mitigation - A review, Anti-Corros. Methods Mater. (2016) 1–40.
[129] Y. T. Al-janabi, "An Overview of Corrosion in Oil and Gas Industry : Upstream , Midstream , and Downstream Sectors," in *Corrosion Inhibitors in the Oil and Gas Industry*, 1st editio., V. S. Saji and S. A. Umoren, Eds. Germany: Wiley-VCHVerlag GmbH& Co. KGaA, 2020, pp. 1–38.
[130] M. Baker, R.R. Fessler, "pipeline Corrosion" (2008).
[131] D.E.P. Klenam, L.H. Chown, M.J. Papo, L.A. Cornish, Steels for rail axles - an overview, in: Critical Reviews in Solid State and Materials Sciences, 2022, pp. 1–32, https://doi.org/10.1080/10408436.2022.2137462.
[132] D.E.P. Klenam, Composition refinement of medium carbon-low alloy steels to improve wear and corrosion resistance for rail axle applications, University of the Witwatersrand, 2019.
[133] M. Ueda, "2006 f. n., Speller Award Lecture : Development of Corrosion-Resistance Alloys for the Oil and Gas Industry — Based on Spontaneous Passivity Mechanism" no. October (2006) 856–867.
[134] N.R. Rundora, J.W. Van der Merwe, D.E.P. Klenam, M.O. Bodunrin, Enhanced corrosion performance of low-cost titanium alloys in a simulated diabetic environment, Mater. Corros. (2023), https://doi.org/10.1002/maco.202313927.
[135] N.D. Tomashov, Passivity and corrosion resistance of metal systems, Corros Sci 4 (1–4) (1964) 315–334, https://doi.org/10.1016/0010-938X(64)90028-9.
[136] A.U. Malik, N.A. Siddiqi, S. Ahmad, I.N. Andijani, The effect of dominant alloy additions on the corrosion behavior of some conventional and high alloy stainless steels in seawater, Corros Sci 37 (10) (1995) 1521–1535, https://doi.org/10.1016/0010-938X(95)00043-J.
[137] H.Y. Ha, T.H. Lee, J.H. Bae, D.W. Chun, Molybdenum effects on pitting corrosion resistance of FeCrMnMoNC austenitic stainless steels, Metals (basel) 8 (8) (2018) 1–13.
[138] H. Luo, C. Dong, K. Xiao, X. Li, The passive behaviour of ferritic stainless steel containing alloyed tin in acidic media, RSC Adv 6 (12) (2016) 9940–9949, https://doi.org/10.1039/c5ra23698c.
[139] J. Bhandari, F. Khan, R. Abbassi, V. Garaniya, R. Ojeda, Modelling of pitting corrosion in marine and offshore steel structures - A technical review, J Loss Prev Process Ind 37 (2015) 39–62, https://doi.org/10.1016/j.jlp.2015.06.008.
[140] J.D. Henderson, X. Li, D.W. Shoesmith, J.J. Noël, K. Ogle, Molybdenum surface enrichment and release during transpassive dissolution of Ni-based alloys, Corros Sci 147 (Feb. 2019) 32–40, https://doi.org/10.1016/j.corsci.2018.11.005.
[141] Y.T. Sun, X. Tan, L.L. Lei, J. Li, Y.M. Jiang, Revisiting the effect of molybdenum on pitting resistance of stainless steels, Tungsten 3 (3) (Sep. 2021) 329–337, https://doi.org/10.1007/s42864-021-00099-1.
[142] M. Ma, C. He, L. Chen, L. Wei, R.D.K. Misra, Effect of W and Ce additions on the electrochemical corrosion behaviour of 444-type ferritic stainless steel, Corros. Eng. Sci. Technol. 53 (3) (Apr. 2018) 199–205, https://doi.org/10.1080/1478422X.2018.1429701.
[143] J.B. Lee, Effects of alloying elements, Cr, Mo and N on repassivation characteristics of stainless steels using the abrading electrode technique, Mater Chem Phys 99 (2–3) (Oct. 2006) 224–234, https://doi.org/10.1016/j.matchemphys.2005.10.016.
[144] K. Sugimoto, Y. Sawada, The role of molybdenum additions to austenitic stainless steels in the inhibition of pitting in acid chloride solutions, Corros Sci 17 (1977) 425–445.
[145] K.M. Jung, S.H. Ahn, Y.J. Kim, S.K. Oh, W.H. Ryu, H.S. Kwon, Alloy design employing high Cr concentrations for Mo-free stainless steels with enhanced corrosion resistance, Corros Sci 140 (Aug. 2018) 61–72, https://doi.org/10.1016/j.corsci.2018.06.021.
[146] S.L. Sorensen, X. Zheng, S.H. Southworth, Surface Composition of Stainless Steels during Anodic Dissolution and Passivation, J Electrochem Soc 132 (12) (1985) 2854–2861.
[147] C. Loable, I.N. Viçosa, T.J. Mesquita, M. Mantel, R.P. Nogueira, G. Berthomé, E. Chauveau, V. Roche, Synergy between molybdenum and nitrogen on the pitting corrosion and passive film resistance of austenitic stainless steels as a pH-dependent effect, Mater Chem Phys 186 (Jan. 2017) 237–245, https://doi.org/10.1016/j.matchemphys.2016.10.049.
[148] K. Hashimoto, K. Asami, K. Teramoto, An x-ray photo-electron spectroscopy study on the role of Mo in increasing the corrosion resistance of ferritic stainless steels in HCl, Corros Sci 19 (1979) 3–14.
[149] T.J. Mesquita, E. Chauveau, M. Mantel, N. Kinsman, V. Roche, R.P. Nogueira, Lean duplex stainless steels-The role of molybdenum in pitting corrosion of concrete reinforcement studied with industrial and laboratory castings, Mater Chem Phys 132 (2–3) (Feb. 2012) 967–972, https://doi.org/10.1016/j.matchemphys.2011.12.042.

[150] J.R. Galvele, J.B. Lumsden, R.W. Staehle, Effect of molybdenum on the pitting potential of high purity 18% Cr ferritic stainless steels, Journal of the Eletrochemical Society 125 (8) (1968) 1204–1208.
[151] T.J. Mesquita, E. Chauveau, M. Mantel, R.P. Nogueira, A XPS study of the Mo effect on passivation behaviors for highly controlled stainless steels in neutral and alkaline conditions, Appl Surf Sci 270 (Apr. 2013) 90–97, https://doi.org/10.1016/j.apsusc.2012.12.118.
[152] D.E.P. Klenam, P. Claudia, L.C. Chown, S. Kwofie, L.A. Cornish, "Mechanical behaviour of pack carburized AISI 316L austenitic stainless steel", The, J. South Afr. Inst. Min. Metall. 115 (12) (2015) 1183–1191.
[153] R. Karimi Shervedani, A. Lasia -Physical, N. Kumagai, T. Fujiwara, and K. Tanno,, Determination of the Minimum Surface Enrichment of Molybdenum Required to Inhibit Active Dissolution of an Fe-Cr-Ni-Mo Alloy, J Electrochem Soc 131 (1) (1984) 223–225.
[154] J.N. Wanklyn, The role of molybdenum in the crevice corrosion of stainless steels, Corros Sci 21 (3) (1981) 211–225.
[155] M.A. Domínguez-Aguilar, R.C. Newman, Detection of deleterious phases in duplex stainless steel by weak galvanostatic polarization in halide solutions, Corros Sci 48 (9) (Sep. 2006) 2577–2591, https://doi.org/10.1016/j.corsci.2005.08.018.
[156] W. Yang, R.-C. Ni, H.-Z. Hua, A. Pourbaix, The behaviour of chromium and molybdenum in the propagation process of localized corrosion of steels, Corros Sci 24 (8) (1984) 691–707.
[157] R.K. Gupta, N. Birbilis, The influence of nanocrystalline structure and processing route on corrosion of stainless steel: A review, Corros Sci 92 (2015) 1–15, https://doi.org/10.1016/j.corsci.2014.11.041.
[158] B. J. Kagay, "Hydrogen embrittlement testing of alloy 718 for oil and gas applications," p. 105, 2016.
[159] H. S. Klapper, J. Klöwer, and O. Gosheva, "Hydrogen embrittlement: The game changing factor in the applicability of nickel alloys in oilfield technology," *Philosophical Transactions of the Royal Society A: Mathematical, Physical and Engineering Sciences*, vol. 375, no. 2098, Jul. 2017, doi: 10.1098/rsta.2016.0415.
[160] E.C. Bain, W.E. Griffiths, "An introduction to the iron-chromium-nickel alloys", Transactions of American Institute of Mineral and Metallurgical, Engineering 75 (1927) 166–213.
[161] D.G. Kolman, A review of the potential environmentally assisted failure mechanisms of austenitic stainless steel storage containers housing stabilized radioactive compounds, Corros Sci 43 (1) (2001) 99–125, https://doi.org/10.1016/S0010-938X(00)00061-5.
[162] M. H. Wood, A. V. Arellano, and L. Van Wijk, "Corrosion-Related Accidents in Petroleum Refineries: Lessons learned from accidents in EU and OECD countries," 2013.
[163] L.M. Branscomb, Networks for the nineties, IEEE Commun. Mag. 21 (7) (1983) 38–43, https://doi.org/10.1109/MCOM.1983.1091466.
[164] D.E.P. Klenam, N. Rahbar, W.O. Soboyejo, "Mechanical Properties of Complex Concentrated Alloys: Implications for Structural Integrity", in Reference Module in Materials Science and Materials Engineering, Elsevier (2022), https://doi.org/10.1016/B978-0-12-822944-6.00047-5.
[165] O. Akinbami, L. Mohlala, D.E.P. Klenam, J. van der Merwe, M. Bodunrin, The status of high entropy alloys studies in Africa : an Overview, Key Eng Mater 917 (2022) 41–53.
[166] D. E. P. Klenam, G. Egowan, M. O. Bodunrin, J. W. van der Merwe, N. Rahbar, and W. O. Soboyejo, "Complex Concentrated Alloys: A Cornucopia of Possible Structural and Functional Applications," in *Comprehensive Structural Integrity*, vol. 2, Elsevier, 2023, pp. 50–90. doi: 10.1016/B978-0-12-822944-6.00056-6.
[167] M. Tsai and J. Yeh, "High-Entropy Alloys : A Critical Review High-Entropy Alloys : A Critical Review," no. April, 2014, doi: 10.1080/21663831.2014.912690.
[168] D.E.P. Klenam, N. Rahbar, W.O. Soboyejo, "Critical Review of Limitations of Equiatomic Composition Alloying Strategy of Complex Concentrated Alloys", in Comprehensive Structural Integrity, Elsevier 2 (2023) 122–135, https://doi.org/10.1016/B978-0-12-822944-6.00055-4.
[169] D.E.P. Klenam, N. Rahbar, W.O. Soboyejo, "Critical Review of Factors Hindering Scalability of Complex Concentrated Alloys", in Comprehensive Structural Integrity, Elsevier 2 (2023) 103–121, https://doi.org/10.1016/B978-0-12-822944-6.00051-7.
[170] E.J. Pickering, N.G. Jones, High-entropy alloys: a critical assessment of their founding principles and future prospects, Int. Mater. Rev. 61 (3) (2016) 183–202.
[171] M. Tsai, J. Yeh, M. Tsai, J. Yeh, High-Entropy Alloys : A Critical Review, Mater Res Lett 2 (3) (2014) 107–123.
[172] D.B. Miracle, O.N. Senkov, A critical review of high entropy alloys and related concepts, Acta Mater 122 (2017) 448–511.
[173] Y. Zhang, T. Ting, Z. Tang, M. C. Gao, K. A. Dahmen, P. K. Liaw, and Z. Ping, "Progress in Materials Science Microstructures and properties of high-entropy alloys," *Prog Mater Sci*, vol. 61, no. September 2013, pp. 1–93, 2014, doi: 10.1016/j.pmatsci.2013.10.001.
[174] X. Chang, M. Zeng, K. Liu, and L. Fu, "Phase Engineering of High-Entropy Alloys," *Advanced Materials*, vol. 32, no. 14. Wiley-VCH Verlag, Apr. 01, 2020. doi: 10.1002/adma.201907226.
[175] D.E.P. Klenam, N. Rahbar, W.O. Soboyejo, "Mechanical Properties of Complex Concentrated Alloys: Implications for Structural Integrity", in Comprehensive Structural Integrity, Elsevier 2 (2023) 209–239, https://doi.org/10.1016/B978-0-12-822944-6.00047-5.
[176] M. Leshetla, D.E.P. Klenam, J.W. van der Merwe, D. Whitefield, M.O. Bodunrin, H. Potgieter, Corrosion resistance of iron - containing experimental titanium alloys exposed to simulated body fluids, Mater. Corros. (2022) 1–10.
[177] S.A. Kube, J. Schroers, Metastability in high entropy alloys, Scr Mater 186 (2020) 392–400.
[178] K. Liu, S.S. Nene, M. Frank, S. Sinha, R.S. Mishra, Metastability-assisted fatigue behavior in a friction stir processed dual-phase high entropy alloy, Mater Res Lett 6 (11) (2018) 613–619.
[179] S. Wei, F. He, C.C. Tasan, Metastability in high-entropy alloys: A review, J Mater Res 33 (19) (2018) 2924–2937.
[180] S. Zhu, D. Yan, K. Gan, W. Lu, Z. Li, Awakening the metastability of an interstitial high entropy alloy via severe deformation, Scr Mater 191 (2021) 96–100.
[181] H. Huang, Y. Wu, J. He, H. Wang, X. Liu, K. An, W. Wu, Z. Lu, Phase-Transformation Ductilization of Brittle High-Entropy Alloys via Metastability Engineering, Adv. Mater. 29 (30) (2017) 1–7, https://doi.org/10.1002/adma.201701678.
[182] Y. Fu, J. Li, H. Luo, C. Du, X. Li, Recent advances on environmental corrosion behavior and mechanism of high-entropy alloys, J Mater Sci Technol 80 (2021) 217–233.
[183] B.X. Cao, C. Wang, T. Yang, C.T. Liu, Cocktail effects in understanding the stability and properties of face-centered-cubic high-entropy alloys at ambient and cryogenic temperatures, Scr Mater 187 (2020) 250–255.
[184] V. Firouzdor, K. Sridharan, G. Cao, M. Anderson, T.R. Allen, Corrosion of a stainless steel and nickel-based alloys in high temperature supercritical carbon dioxide environment, Corros Sci 69 (2013) 281–291.
[185] P. Crook, Corrosion resistant nickel alloys, Adv. Mater. Process. 165 (8) (2007) 45–48.
[186] G.O. Ilevbare, G.T. Burstein, The inhibition of pitting corrosion of stainless steels by chromate and molybdate ions, Corros Sci 45 (7) (2003) 1545–1569.
[187] P.I. Marshall, G.T. Burstein, Effects of alloyed molybdenum on the kinetics of repassivation on austenitic stainless steels, Corros Sci 24 (5) (1984) 463–478.
[188] R.C. Newman, The dissolution and passivation kinetics of stainless alloys containing molybdenum-II. Dissolution kinetics in artificial pits, Corros Sci 25 (5) (1985) 341–350.
[189] I. Baker, Interstitials in f.c.c. high entropy alloys, Metals (basel) 10 (5) (2020) 1–20.
[190] Z. Su, J. Ding, M. Song, L. Jiang, T. Shi, Z. Li, S. Wang, F. Gao, D. Yun, C. Lu, and E. Ma, "Radiation-tolerant high-entropy alloys via interstitial-solute-induced chemical heterogeneities," no. March, 2021, [Online]. Available: http://arxiv.org/abs/2103.15134.
[191] J. Svoboda, W. Ecker, V. I. Razumovskiy, G. A. Zickler, and F. D. Fischer, "Kinetics of interaction of impurity interstitials with dislocations revisited," *Prog Mater Sci*, vol. 101, no. October 2018, pp. 172–206, 2019, doi: 10.1016/j.pmatsci.2018.10.001.
[192] Z. He, Y. Guo, L. Sun, H. Le Yan, X. Guan, S. Jiang, Y. Shen, W. Yin, X. Zhao, Z. Li, N. Jia, Interstitial-driven local chemical order enables ultrastrong face-centered cubic multicomponent alloys, Acta Mater 243 (Jan. 2023), https://doi.org/10.1016/j.actamat.2022.118495.
[193] Y. Ma, X. Liu, W. Dong, R. Li, Y. Zhang, Y. Lu, P. Yu, G. Li, Interstitial carbide synergistically strengthening high-entropy alloy CoCrFeNiV0.5Cx, Mater. Sci. Eng. A 792 (Aug. 2020) 139802.
[194] I. Moravcik, N.S. Peighambardoust, A. Motallebzadeh, L. Moravcikova-Gouvea, C. Liu, J.M. Prabhakar, I. Dlouhy, Z. Li, Interstitial nitrogen enhances corrosion resistance of an equiatomic CoCrNi medium-entropy alloy in sulfuric acid solution, Mater Charact 172 (2021) 110869.
[195] Z. Li, C.C. Tasan, H. Springer, B. Gault, D. Raabe, Interstitial atoms enable joint twinning and transformation induced plasticity in strong and ductile high-entropy alloys, Sci Rep 7 (January) (2017) 1–7.

[196] Y. Liu, G.P. Zheng, M. Li, The effects of short-range chemical and structural ordering related to oxygen interstitials on mechanical properties of CrCoFeNi high-entropy alloys: A first-principles study, J Alloys Compd 843 (2020) 156060.
[197] Z. Wang, I. Baker, Z. Cai, S. Chen, J.D. Poplawsky, W. Guo, The effect of interstitial carbon on the mechanical properties and dislocation substructure evolution in Fe40.4Ni11.3Mn34.8Al7.5Cr6 high entropy alloys, Acta Mater 120 (2016) 228–239.
[198] Z. Fu, P. Wu, S. Zhu, K. Gan, D. Yan, and Z. Li, "Effects of interstitial C and N on hydrogen embrittlement behavior of non-equiatomic metastable FeMnCoCr high-entropy alloys," *Corros Sci*, vol. 194, no. November 2021, p. 109933, 2022.
[199] K. Gan, D. Yan, S. Zhu, Z. Li, Interstitial effects on the incipient plasticity and dislocation behavior of a metastable high-entropy alloy: Nanoindentation experiments and statistical modeling, Acta Mater 206 (2021) 116633.
[200] B. Hwang, T.-H. Lee, S.-J. Kim, Effect of alloying elements on ductile-to-brittle transition behavior of high-interstitial-alloyed 18Cr-10Mn austenitic steels, Procedia Eng 10 (2011) 409–414.
[201] M.C. Gao, J.W. Yeh, P.K. Liaw, Y. Zhang, High-Entropy Alloys: Fundamentals and Applications, 1st ed., Springer International Publishing, 2016.
[202] A.A. Rempel, B. R. Gel'Chinskii,, High-entropy alloys: Preparation, properties and practical application, Izvestiya Ferrous Metallurgy 63 (3–4) (2020) 248–253, https://doi.org/10.17073/0368-0797-2020-3-4-248-253.
[203] B.S. Murty, J.W. Yeh, S. Ranganathan, High-Entropy Alloys, Butterworth-Heinemann, London, UK, 2014.
[204] N. Birbilis, S. Choudhary, J.R. Scully, M.L. Taheri, A perspective on corrosion of multi-principal element alloys, Npj Mater Degrad 5 (1) (2021) 1–8.
[205] W. Zhang, P.K. Liaw, Y. Zhang, Science and technology in high-entropy alloys, Sci China Mater 61 (1) (2018) 2–22.
[206] Y. Qiu, S. Thomas, M.A. Gibson, H.L. Fraser, K. Pohl, N. Birbilis, Microstructure and corrosion properties of the low-density single-phase compositionally complex alloy AlTiVCr, Corros Sci 133 (October) (2017, 2018,) 386–396.
[207] Y.Y. Chen, T. Duval, U.D. Hung, J.W. Yeh, H.C. Shih, Microstructure and electrochemical properties of high entropy alloys-a comparison with type-304 stainless steel, Corros Sci 47 (9) (2005) 2257–2279.
[208] Y. Yu, S. Shironita, K. Souma, M. Umeda, Effect of chromium content on the corrosion resistance of ferritic stainless steels in sulfuric acid solution, Heliyon 4 (11) (2018) e00958.
[209] S. Xuliang, W. Zhijun, H. E. Feng, W. Jincheng, L. I. Junjie, and Y. U. Jiakang, "The intrinsic mechanism of corrosion resistance for FCC high entropy alloys," pp. 1–8, 2017, doi: 10.1007/s11431-017-9114-1.
[210] B. Ren, Z.X. Liu, D.M. Li, L. Shi, B. Cai, M.X. Wang, Corrosion behavior of CuCrFeNiMn high entropy alloy system in 1 M sulfuric acid solution, Mater. Corros. 63 (9) (2012) 828–834.
[211] Y.Q. Jiang, J. Li, Y.F. Juan, Z.J. Lu, W.L. Jia, Evolution in microstructure and corrosion behavior of AlCoCr x FeNi high-entropy alloy coatings fabricated by laser cladding, J Alloys Compd 775 (2019) 1–14.
[212] Z. H. I. Tang, M. C. Gao, H. Diao, T. Yang, J. Liu, T. Zuo, Y. Zhang, Z. Lu, Y. Cheng, Y. Zhang, K. A. Dahmen, P. K. Liaw, and T. Egami, "Aluminum Alloying Effects on Lattice Types , Microstructures , and Mechanical Behavior of High-Entropy Alloys Systems," pp. 17–21, 2013, doi: 10.1007/s11837-013-0776-z.
[213] X. Ye, M. Ma, Y. Cao, W. Liu, X. Ye, Y. Gu, The property research on high-entropy alloy AlxFeCoNiCuCr coating by laser cladding, Phys Procedia vol. 12, no. PART 1 (2011) 303–312, https://doi.org/10.1016/j.phpro.2011.03.039.
[214] C.M. Lin, H.L. Tsai, Evolution of microstructure, hardness, and corrosion properties of high-entropy Al0.5CoCrFeNi alloy, Intermetallics (barking) 19 (3) (2011) 288–294, https://doi.org/10.1016/j.intermet.2010.10.008.
[215] C.P. Lee, C.C. Chang, Y.Y. Chen, J.W. Yeh, H.C. Shih, The corrosion behaviour in aqueous environments, Corros Sci 50 (2008) 2053–2060.
[216] Y.F. Kao, T.D. Lee, S.K. Chen, Y.S. Chang, Electrochemical passive properties of AlxCoCrFeNi (x = 0, 0.25, 0.50, 1.00) alloys in sulfuric acids, Corros Sci 52 (3) (2010) 1026–1034, https://doi.org/10.1016/j.corsci.2009.11.028.
[217] C. Lin, H. Tsai, H. Bor, Effect of aging treatment on microstructure and properties of high-entropy Cu0.5CoCrFeNi alloy, Intermetallics (barking) 18 (6) (2010) 1244–1250.
[218] C.P. Lee, Y.Y. Chen, C.Y. Hsu, J.W. Yeh, H.C. Shih, Enhancing pitting corrosion resistance of AlxCrFe1.5MnNi0.5 high-entropy alloys by anodic treatment in sulfuric acid, Thin Solid Films 517 (3) (2008) 1301–1305.
[219] C. Zhang, G.J. Chen, P.Q. Dai, Evolution of the microstructure and properties of laser-clad FeCrNiCoBx high-entropy alloy coatings, Mater. Sci. Technol. 32 (16) (2016) 1666–1672.
[220] Z.Y. Zheng, X.C. Li, C. Zhang, J.C. Li, Microstructure and corrosion behaviour of FeCoNiCuSnx high entropy alloys, Materials Science and Technology (united Kingdom) 31 (10) (2015) 1148–1152.
[221] X.W. Qiu, Microstructure and properties of AlCrFeNiCoCu high entropy alloy prepared by powder metallurgy, J Alloys Compd 555 (2013) 246–249.
[222] J.B. Cheng, X.B. Liang, B.S. Xu, Effect of Nb addition on the structure and mechanical behaviors of CoCrCuFeNi high-entropy alloy coatings, Surf Coat Technol 240 (2014) 184–190.
[223] R.B. Nair, H.S. Arora, A. Ayyagari, S. Mukherjee, H.S. Grewal, High Entropy Alloys: Prospective Materials for Tribo-Corrosion Applications, Adv Eng Mater 20 (6) (2018) 1–9.
[224] L. Gao, W. Liao, H. Zhang, J.U. Surjadi, D. Sun, Y. Lu, Microstructure, mechanical and corrosion behaviors of CoCrFeNiAl 0.3 High Entropy Alloy (HEA) films, Coatings 7 (10) (2017) 1–7.
[225] Y. Shi, B. Yang, X. Xie, J. Brechtl, K.A. Dahmen, P.K. Liaw, Corrosion of Al xCoCrFeNi high-entropy alloys: Al-content and potential scan-rate dependent pitting behavior, Corros Sci 119 (2017) 33–45.
[226] T.S. Srivatsan, M. Gupta, High entropy alloys - Innovations, advances, and Applications, 1st Edn., Taylor & Francis Group, Boca Raton, 2020.
[227] S. Zhang, C.L. Wu, C.H. Zhang, M. Guan, J.Z. Tan, Laser surface alloying of FeCoCrAlNi high-entropy alloy on 304 stainless steel to enhance corrosion and cavitation erosion resistance, Opt Laser Technol 84 (2016) 23–31.
[228] Q.H. Li, T.M. Yue, Z.N. Guo, X. Lin, Microstructure and corrosion properties of alcocrfeni high entropy alloy coatings deposited on AISI 1045 steel by the electrospark process, Metall Mater Trans A Phys Metall Mater Sci 44 (4) (2013) 1767–1778.
[229] Y. Shon, S.S. Joshi, S. Katakam, R.S. Rajamure, N.B. Dahotre, Laser additive synthesis of high entropy alloy coating on aluminum: Corrosion behavior, Mater Lett 142 (2015) 122–125.
[230] C.P. Lee, Y.Y. Chen, C.Y. Hsu, J.W. Yeh, H.C. Shih, The Effect of Boron on the Corrosion Resistance of the High Entropy Alloys Al0.5CoCrCuFeNiBx, J Electrochem Soc 154 (8) (2007) C424–C430.
[231] Y.L. Chou, J.W. Yeh, H.C. Shih, The effect of molybdenum on the corrosion behaviour of the high-entropy alloys Co 1. 5 CrFeNi 1. 5 Ti 0. 5 Mo x in aqueous environments, Corros Sci 52 (8) (2010) 2571–2581.
[232] X. Ye, M. Ma, Y. Cao, W. Liu, X. Ye, Y. Gu, The property research on high-entropy alloy AlxFeCoNiCuCr coating by laser cladding, Phys Procedia 12 (2011) 303–312.
[233] J.B. Cheng, X.B. Liang, Z.H. Wang, B.S. Xu, Formation and mechanical properties of conicufecr high-entropy alloys coatings prepared by plasma transferred arc cladding process, Plasma Chem. Plasma Process. 33 (5) (2013) 979–992.
[234] B. Li, K. Peng, A. Hu, L. Zhou, J. Zhu, D. Li, Structure and properties of FeCoNiCrCu0.5Alx high-entropy alloy, Trans. Nonferrous Met. Soc. Chin. 23 (3) (2013) 735–741.
[235] J.J. Zhang, X.L. Yin, Y. Dong, Y.P. Lu, L. Jiang, T.M. Wang, T.J. Li, Corrosion properties of AlxCoCrFeNiTi0·5 high entropy alloys in 0·5M H2SO4 aqueous solution, Mater. Res. Innov. 18 (2014) S4756–S4760.
[236] D. Liu, J.B. Cheng, H. Ling, Electrochemical behaviours of (NiCoFeCrCu)95B5 high entropy alloy coatings, Mater. Sci. Technol. 31 (10) (2015) 1159–1164.
[237] C.W. Lin, M.H. Tsai, C.W. Tsai, J.W. Yeh, S.K. Chen, Microstructure and aging behaviour of Al5Cr32Fe35Ni22Ti6 high entropy alloy, Mater. Sci. Technol. 31 (10) (2015) 1165–1170.
[238] D.H. Xiao, P.F. Zhou, W.Q. Wu, H.Y. Diao, M.C. Gao, M. Song, P.K. Liaw, Microstructure, mechanical and corrosion behaviors of AlCoCuFeNi-(Cr, Ti) high entropy alloys, Mater Des 116 (2017) 438–447.

[239] J. Ding, A. Inoue, Y. Han, F.L. Kong, S.L. Zhu, Z. Wang, E. Shalaan, F. Al-Marzouki, High entropy effect on structure and properties of (Fe Co, Ni, Cr)-B amorphous alloys, J Alloys Compd 696 (2017) 345–352.
[240] J. Jayaraj, C. Thinaharan, S. Ningshen, C. Mallika, U. Kamachi Mudali, Corrosion behavior and surface film characterization of TaNbHfZrTi high entropy alloy in aggressive nitric acid medium, Intermetallics (barking) 89 (2017) 123–132.
[241] B. Wang, J. Huang, J. Fan, Y. Dou, H. Zhu, D. Wang, Preparation of FeCoNiCrMn High Entropy Alloy by Electrochemical Reduction of Solid Oxides in Molten Salt and Its Corrosion Behavior in Aqueous Solution, J Electrochem Soc 164 (14) (2017) E575–E579.
[242] Q.H. Li, T.M. Yue, Z.N. Guo, X. Lin, Microstructure and corrosion properties of alcocrfeni high entropy alloy coatings deposited on AISI 1045 steel by the electrospark process, Metall Mater Trans A Phys Metall Mater Sci 44A (2013) 1767–1778.
[243] W. Chai, T. Lu, and Y. Pan, "Corrosion behaviors of FeCoNiCrx (x = 0, 0.5, 1.0) multi-principal element alloys: Role of Cr-induced segregation," *Intermetallics (Barking)*, vol. 116, no. July 2019, p. 106654, 2020, doi: 10.1016/j.intermet.2019.106654.
[244] Y. Qiu, S. Thomas, M. A. Gibson, H. L. Fraser, and N. Birbilis, "Corrosion of high entropy alloys," *npj Materials Degradation*, vol. 1, no. 1. Nature, Dec. 01, 2017. doi: 10.1038/s41529-017-0009-y.
[245] B. Ren, Z.X. Liu, D.M. Li, L. Shi, B. Cai, M.X. Wang, Corrosion behavior of CuCrFeNiMn high entropy alloy system in 1 M sulfuric acid solution, Mater. Corros. 63 (9) (Sep. 2012) 828–834, https://doi.org/10.1002/maco.201106072.
[246] Y. L. Chou, J. W. Yeh, and H. C. Shih, "Effect of Molybdenum on the Pitting Resistance of Co1.5CrFeNi1.5Ti0.5Mox Alloys in Chloride Solutions," *Corrosion*, vol. 67, no. 8, pp. 085002-1-085002–6, 2011.
[247] X.W. Qiu, Y.P. Zhang, C.G. Liu, Effect of Ti content on st ructure and properties of Al 2 CrFeNiCoCuTi x high-entropy alloy coatings, J Alloys Compd (2013), https://doi.org/10.1016/j.jallcom.2013.09.083.
[248] L. Huang, X. J. Wang, B. X. Huang, and C. Z. Wang, "Study on Microstructure and Corrosion Resistance of AlCoCrFeNiTi (x) High-Entropy Alloys," no. x, 2020, doi: 10.1088/1757-899X/774/1/012058.
[249] M. Vandadi, D. E. P. Klenam, N. Rahbar, and W. O. Soboyejo, "Advances in the Structural Integrity of Cold Sprayed Alloys - A Critical Review of Process Models and Mechanical Properties," in *Comprehensive Structural Integrity*, vol. 2, Elsevier Ltd., 2023, pp. 2–37. doi: 10.1016/b978-0-12-822944-6.00049-9.
[250] D. Klenam, T. Asumadu, M. Bodunrin, M. Vandadi, T. Bond, J. van der Merwe, N. Rahbar, W. Soboyejo, Cold Spray Coatings of Complex Concentrated Alloys: Critical Assessment of Milestones, Challenges, and Opportunities, Coatings 13 (538) (2023) 1–50.
[251] S. Wang, H. Ye, "first-Principles Studies on the Component Dependences of High-Entropy Alloys" 338 (2011) 380–383.
[252] G. Salvago, G. Fumagalli, D. Sinigaglia, The corrosion behaviour of AISI 304L stainless steel in 0.1 M HCl at room temperature-I, Corros Sci 23 (5) (1983) 507–514, https://doi.org/10.1016/0010-938X(83)90100-2.
[253] M. Ma, X. Ye, W. Liu, L. Li, M. Zhong, Y. Liu, Q. Wu, Synthesis and characterization of high-entropy alloy Al Xfeconicucr by laser cladding, Adv. Mater. Sci. Eng. 2011 (2011), https://doi.org/10.1155/2011/485942.
[254] D.E.P. Klenam, T.K. Asumadu, M. Vandadi, N. Rahbar, F. McBagonluri, W.O. Soboyejo, Data science and material informatics in physical metallurgy and material science: An overview of milestones and limitations, Results in Materials 19 (2023), https://doi.org/10.1016/j.rinma.2023.100455.